**ANA RAQUEL SANTOS PEREIRA**
Licenciada em Biologia Celular e Molecular

# ADIPOCYTE METABOLIC RESPONSE TO *TRYPANOSOMA BRUCEI* IN A CO-CULTURE SETTING

MESTRADO EM MICROBIOLOGIA MÉDICA
Universidade NOVA de Lisboa
Novembro, 2021

**ANA RAQUEL SANTOS PEREIRA**
Licenciada em Biologia Celular e Molecular

# ADIPOCYTE METABOLIC RESPONSE TO *TRYPANOSOMA BRUCEI* IN A CO-CULTURE SETTING

MESTRADO EM MICROBIOLOGIA MÉDICA
Universidade NOVA de Lisboa
Novembro, 2021

# ADIPOCYTE METABOLIC RESPONSE TO *TRYPANOSOMA BRUCEI* IN A CO-CULTURE SETTING

**ANA RAQUEL SANTOS PEREIRA**

Licenciada em Biologia Celular e Molecular

**Orientador:** Luísa Miranda Figueiredo, PhD,
Instituto de Medicina Molecular-João Lobo Antunes

**Coorientador:** Mónica Serrano, PhD,
Instituto de Tecnologia Química e Biológica António Xavier

**Júri:**

**Presidente:** José Paulo Sampaio,
Professor Associado com Agregação, FCT-NOVA

**Arguente:** Vanessa Zuzarte Luís,
Chief Molecular Scientist, SGS Portugal

**Orientador:** Luísa Miranda Figueiredo,
Professora Associada Convidada, iMM-JLA

MESTRADO EM MICROBIOLOGIA MÉDICA

Universidade NOVA de Lisboa
Novembro, 2021

**Adipocyte metabolic response to *Trypanosoma brucei* in a co-culture setting.**

# Acknowledgements

Em primeiro lugar, queria agradecer à Luísa por me ter recebido no seu laboratório e pela oportunidade de entrar no mundo dos tripanossomas! Agradeço a orientação, os conselhos e a disponibilidade durante todo o desenvolvimento deste trabalho.

Agradeço também à Drª. Mónica Serrano, por ter aceitado ser minha coorientadora.

Ao Henrique, por toda a orientação durante o desenvolvimento desta tese. Agradeço a partilha de tempo e conhecimento, sempre rigorosa, mas nunca aborrecida. Obrigada pelas discussões acompanhadas de boa disposição, pela constante disponibilidade para responder às minhas questões (mesmo quando me esquecia que já as tinha preguntado), paciência, compreensão, amizade e filosofia de vida (eheh). Estou eternamente grata!

A todo o grupo: Adriana, Fabien, Idálio, Lara, Leonor, Lúcia, Sara e Sandra. Pelas novas amizades, pelos momentos de ócio e diversão, pelo companheirismo, motivação, entreajuda e disponibilidade. Vou ter muitas saudades!

Aos amigos de Microbiologia Médica: Filipe, Laura e Lourenço. As noitadas no kaleido nem pareciam tão más na vossa companhia. Obrigada por todos os momentos, não teria sido o mesmo mestrado sem vocês. Foi um prazer partilhar este caminho!

A todos os meus amigos, principalmente: Bea, Caio, Inês, Maria, Marta, Joana e Sara. Que me acompanham nos maus momentos e que são responsáveis pelos melhores também. Obrigada por serem amigas fantásticas e me motivarem a ser e fazer melhor, pessoalmente e profissionalmente.

Aos meus pais, Clara e João, por tudo: a compreensão, o carinho, o apoio e o amor incondicional. Por me lembrarem todos os dias o privilégio de ter uma educação.

# Abstract

African trypanosomiasis is a vector-borne disease caused by extracellular protozoan parasites, including *Trypanosoma brucei*. The establishment of infection in mammalian hosts is characterized by invasion of the bloodstream and solid tissues. Among these, the adipose tissue (AT) is heavily colonized by *T. brucei* in mice. During infection there is also a large reduction of AT mass which suggests the mobilization of lipids stored in the adipocyte. However, it is not known how adipocyte to parasite interactions may contribute to adipocyte lipid metabolism. Here we show that co-culturing 3T3-L1 adipocytes and *T. brucei in vitro* increased adipocyte lipolysis. We found that this increase can be elicited by a soluble parasite factor, but it is larger when live parasites are in direct contact with adipocytes. Furthermore, chemical inhibition of adipose triglyceride lipase (ATGL) during co-culture lead to a reduction of fatty acid and glycerol release, indicating that the release of lipolytic products in the presence of *T. brucei* is an ATGL-dependent mechanism. Overall, the findings in this study indicate that *T. brucei* is able to directly modulate adipocyte catabolism, highlighting the need to further investigate the molecular partners involved in this host-parasite interaction.

**Keywords:** *Trypanosoma brucei*, adipose tissue, lipolysis, 3T3-L1 adipocyte

# Resumo

A tripanossomíase africana é uma doença transmitida por vetores, causada por parasitas protozoários extracelulares, incluindo o *Trypanosoma brucei*. A infeção do hospedeiro mamífero caracteriza-se pela invasão do sistema circulatório e de outros tecidos. Entre estes encontra-se o tecido adiposo, que é extensamente colonizado por *T. brucei* em ratinho. Durante a infeção ocorre uma grande redução da massa do tecido adiposo, sugerindo existir mobilização de lípidos armazenados no adipócito. Contudo, não é conhecido como a interação entre o parasita e o adipócito poderá contribuir para o metabolismo de lípidos no adipócito. Neste estudo demonstramos que num sistema *in vitro* de co-cultura com adipócitos 3T3-L1 e *T. brucei* existe um aumento da lipólise no adipócito. Este aumento pode ser despoletado por um fator solúvel com origem no parasita, no entanto o seu efeito é máximo quando o parasita está viável e em contato direto com o adipócito. Adicionalmente, a inibição química da ATGL durante a co-cultura resulta numa redução da libertação de ácidos gordos e glicerol, indicando que a lipólise induzida por *T. brucei* é dependente da atividade da ATGL. Globalmente, os resultados deste estudo indicam que o *T. brucei* pode modular diretamente o catabolismo do adipócito, realçando a necessidade de investigar os mediadores moleculares envolvidos na interação entre hospedeiro e parasita.

**Palavras-chave:** *Trypanosoma brucei*, tecido adiposo, lipólise, adipócito 3T3-L1

# Table of Contents

# List of Figures

# List of Tables

# List of Abbreviations

| | |
|---|---|
| **3D** | three-dimensional |
| **AAT** | Animal African trypanosomiasis |
| **AC** | Adenylate cyclase |
| **AT** | Adipose tissue |
| **AMPK** | AMP-activated protein kinase |
| **ANOVA** | Analysis of variance |
| **ATF** | Adipose tissue form |
| **ATGL** | Adipose triglyceride lipase |
| **ATP** | Adenosine triphosphate |
| **BAT** | Brown adipose tissue |
| **BCA** | Bicinchoninic acid |
| **BCS** | Bovine calf serum |
| **BSA** | Bovine serum albumin |
| **BSF** | Bloodstream form |
| **cAMP** | Cyclic adenosine monophosphate |
| ***C. burnetii*** | *Coxiella burnetii* |
| **CD36** | Cluster of differentiation 36 |
| **cDNA** | Complementary DNA |
| **CGI-58** | Comparative gene identification-58 |
| **cGMP** | Cyclic guanosine monophosphate |
| **CNS** | Central nervous system |
| **Ct** | Cycle threshold |
| **DAG** | Diacylglycerol |
| **dd$H_2O$** | double-distilled water |
| **DMEM** | Dulbecco's modified Eagle's medium |
| **DMSO** | Dimethyl sulfoxide |
| **DNA** | Deoxyribonucleic acid |
| **ERK** | Extracellular-signal-regulated kinase |
| **ESAG4** | Expression site-associated gene 4 |
| **EV** | Extracellular vesicle |
| **FABP** | Fatty acid-binding protein |
| **FBS** | Fetal bovine serum |
| **G0S2** | G0/G1 switch protein 2 |
| **GAPDH** | Glyceraldehyde 3-phosphate dehydrogenase |

| | |
|---|---|
| **GRESAG4** | Genes related to expression site-associated gene 4 |
| **gWAT** | Gonadal white adipose tissue |
| **HALS** | HIV/antiretroviral therapy-associated lipodystrophy syndrome |
| **HAT** | Human African trypanosomiasis |
| **HIV-1** | Human immunodeficiency virus 1 |
| **HPRT** | Hypoxanthine-guanine phosphoribosyl transferase |
| **HSL** | Hormone-sensitive lipase |
| **IBMX** | 3-isobutyl-1-methylxanthine |
| **IL-6** | Interleukin-6 |
| **JNK** | c-Jun N-terminal kinase |
| **LAL** | Lysosomal acid lipase |
| **LPS** | Lipopolysaccharide |
| **MAG** | Monoacylglycerol |
| **MAPK** | Mitogen-activated protein kinase |
| **MGL** | Monoacylglycerol lipase |
| **mRNA** | Messenger RNA |
| ***M. tuberculosis*** | *Mycobacterium tuberculosis* |
| **NEFA** | Non-esterified fatty acid |
| **NF-κB** | Nuclear factor kappa light chain enhancer of activated B cells |
| **NOD** | Nucleotide-binding oligomerization domain containing protein |
| **NPR-A** | Natriuretic peptide receptor type A |
| **PAD1** | Protein associated with differentiation 1 |
| **PAMP** | Pathogen-associated molecular pattern |
| ***P. berghei*** | *Plasmodium berghei* |
| **PBS** | Phosphate-buffered saline |
| **PDE3B** | Phosphodiesterase 3B |
| **PI3K** | Phosphoinositol-3-kinase |
| **PKA** | Protein kinase A |
| **PKG** | Protein kinase G |
| **PLIN1** | Perilipin-1 |
| **PPARγ** | Peroxisome proliferator-activated receptor γ |
| **PRR** | Pattern recognition receptor |
| **PVDF** | Polyvinylidene fluoride membrane |
| **qPCR** | Quantitative polymerase chain reaction |
| **RBC** | Red blood cell |
| **RIPA** | Radioimmunoprecipitation assay |
| **RNA** | Ribonucleic acid |

| | |
|---|---|
| **rRNA** | Ribosomal RNA |
| ***R. prowazekii*** | *Rickettsia prowazekii* |
| **RT-PCR** | Reverse transcription polymerase chain reaction |
| **SDS-PAGE** | Sodium dodecyl sulphate polyacrylamide gel electrophoresis |
| **SEM** | Standard error of mean |
| **SIF** | Stumpy induction factor |
| ***spp.*** | Species |
| **TAG** | Triacylglycerol |
| ***T. brucei*** | *Trypanosoma brucei* |
| **TBST** | Tris-buffered saline, Tween 20 |
| ***T. congolense*** | *Trypanosoma congolense* |
| ***T. cruzi*** | *Trypanosoma cruzi* |
| **TGS** | Tris-Glycine-SDS |
| **TLR** | Toll-like receptor |
| **TNF-α** | Tumor necrosis factor-α |
| **UCP-1** | Uncoupling protein-1 |
| **Vpr** | Viral protein R |
| **VSG** | Variant surface glycoprotein |
| **WAT** | White adipose tissue |
| **WHO** | World Health Organization |

# 1. Introduction

## 1.1. *Trypanosoma brucei* and African Trypanosomiasis

*Trypanosoma brucei* (*T. brucei*) is an extracellular and unicellular parasite responsible for Human African Trypanosomiasis (HAT), or sleeping sickness in humans, and Animal African Trypanosomiasis (AAT), or nagana in cattle. In 1895, *T. brucei* was identified as the causative agent of nagana by microbiologist David Bruce even though the disease in humans had been earlier described by doctors and medical officers of slave-trade companies[1]. *T. brucei* belongs to the Kinetoplastida order that comprises several flagellated protozoa with a unique DNA-containing organelle within the mitochondria, the kinetoplast[2]. Other known pathogens of medical importance in this group include *Trypanosoma cruzi* (*T. cruzi*) responsible for Chaga's disease and *Leishmania* spp. responsible for leishmaniasis, which unlike *T. brucei* are intracellular parasites[2].

Transmission of the parasite is solely dependent on the tsetse fly (*Glossina* spp.) whose distribution makes HAT and nagana endemic and hence geographically limited to 36 countries in sub-Saharan Africa (Figure 1)[3,4]. HAT is listed by World Health Organization (WHO) as one of 20 neglected tropical diseases[5] and poor rural areas are the most severely affected. Fewer than 1000 new cases were reported in 2019[3] and HAT was targeted for elimination (interruption of transmission to humans) by 2030[5]. Nonetheless, approximately 65 million people are considered at risk and many cases might remain undiagnosed due to scarce resources and political instability[3,5].

HAT has two stages and is lethal if left untreated. The first stage or haemolymphatic stage is accompanied by non-specific symptoms like fever, headache, nausea, generalized pain, night sweats, weight loss and swelling of lymph nodes[6,7]. Here, parasites reside mainly in the bloodstream and lymphatic fluids. In the second stage or meningoencephalitic stage, the parasite crosses the blood-brain barrier and affects the central nervous system (CNS). During this stage an extensive list of symptoms has been described, broadly it encompasses psychiatric, motor and sleep disturbances[8]. Apathy, discoordination, tremors, and inversion of the normal sleep/wake cycle are some of the neurological signs[6,8]. No prophylactic or therapeutic vaccine exists, leaving chemotherapy as the only option for treatment[4,6,8]. Current available drugs are limited and associated with high toxicity, complex administration and variable efficacy. However, collected efforts to develop new drugs culminated in the introduction of fexinidazole for treatment of both stages of Gambiense HAT, in 2018. Fexinidazole is the first orally administered monotherapy for HAT this way simplifying treatment and overcoming administration difficulties[9].

Three morphologically similar sub-species of *T. brucei* have been described. *T. brucei gambiense* and *T. brucei rhodiense* are both responsible for causing HAT, but the disease progresses differently between these sub-species. *T. brucei brucei* causes nagana and is only infective to non-primate mammals.

*T. brucei gambiense* accounts for approximately 95% of reported cases of HAT[3] and the disease has a chronic progression with an average duration of 3 years[4]. While central and western African regions are the main impacted areas of *T. brucei gambiense*, *T. brucei rhodesiense* is the predominant sub-species in East Africa being responsible for the acute form of HAT. Due to the rapid progression of the disease, patients frequently succumb before developing nervous symptoms. Besides infecting humans there is also an important wild animal reservoir which makes this a zoonotic disease and its control more complex[10].

Nagana is caused by many African trypanosomes, which include *Trypanosoma vivax, Trypanosoma congolense* (*T. congolense*) and *T. brucei brucei*[11]. Due to the severity of nagana in domestic livestock, subsistence agriculture and development of the cattle industry in affected countries is hindered and annual losses are estimated to exceed 1 billion USD[10,12].

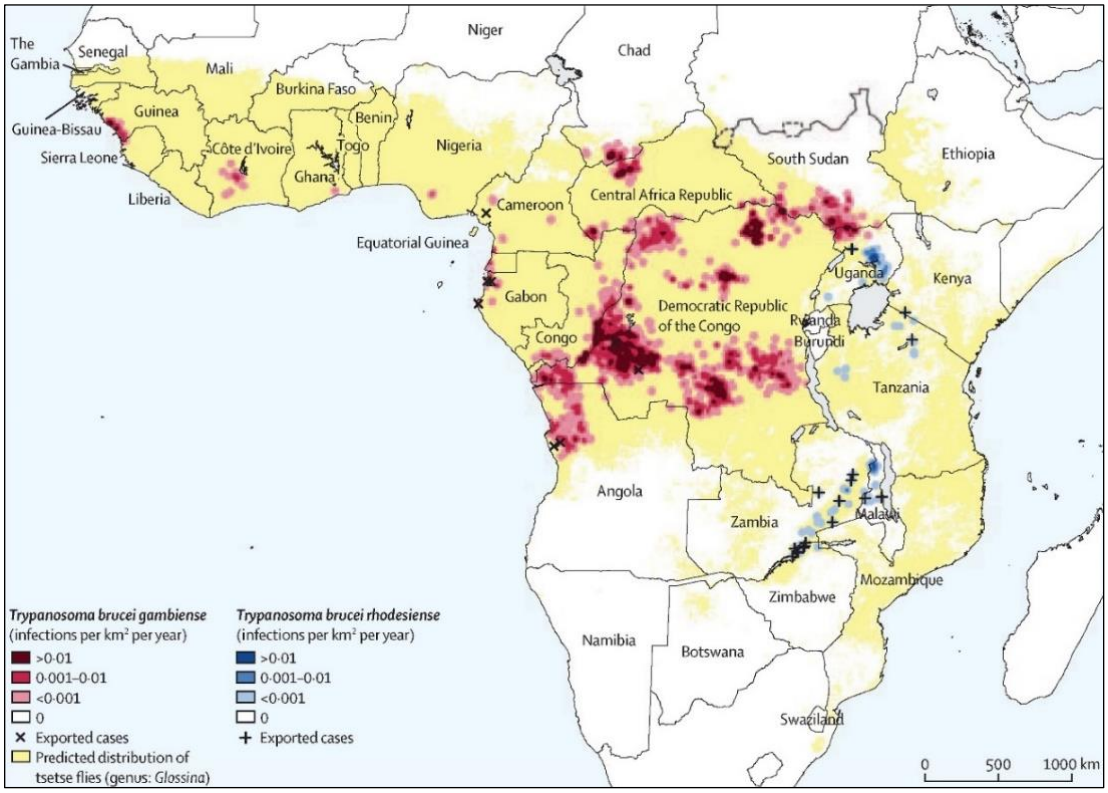


**Figure 1. Geographical distribution of Human African Trypanosomiasis.** The area highlighted in yellow corresponds to the predicted region where tsetse flies of the *Glossina* genus are present, also known as the tsetse belt. In red are represented infections by *T. brucei gambiense*, predominant in central African countries and responsible for the chronic form of HAT. Infections by *T. brucei rhodesiense* are denoted in blue and are present in East Africa. Originally from 4.

### 1.1.1. Life cycle of *Trypanosoma brucei*

The complex life cycle of *T. brucei* alternates between an arthropod vector (tsetse fly) and a mammalian host (Figure 2). To be able to survive in such different environments, the parasite goes through several metabolic and morphological changes[13–15]. Within the mammalian host's bloodstream, *T. brucei* can exist in two forms: the replicative long slender form and the non-replicative short stumpy form which is preadapted to survive in the tsetse fly[13].

During a blood meal, a tsetse fly bites an infected mammal and ingests stumpy forms which then differentiate into procyclic forms in the midgut[13,14]. These procyclic forms divide by binary fission and migrate to the salivary glands where they transform into epimastigotes[14]. After another cycle of divisions, they further differentiate into non-dividing metacyclic forms, which are infective to susceptible vertebrate hosts during the fly's next blood meal[14]. In the blood, metacyclics differentiate into slender forms which replicate rapidly and cause an increase in parasitemia[13].

To avoid killing the host and increase transmission, a large proportion of parasites differentiate into non-replicating stumpy forms[16]. This differentiation is triggered by a density-dependent quorum sensing mechanism mediated by a soluble parasite-derived molecule, the stumpy induction factor (SIF)[17]. This way the start of another transmission cycle can be established.

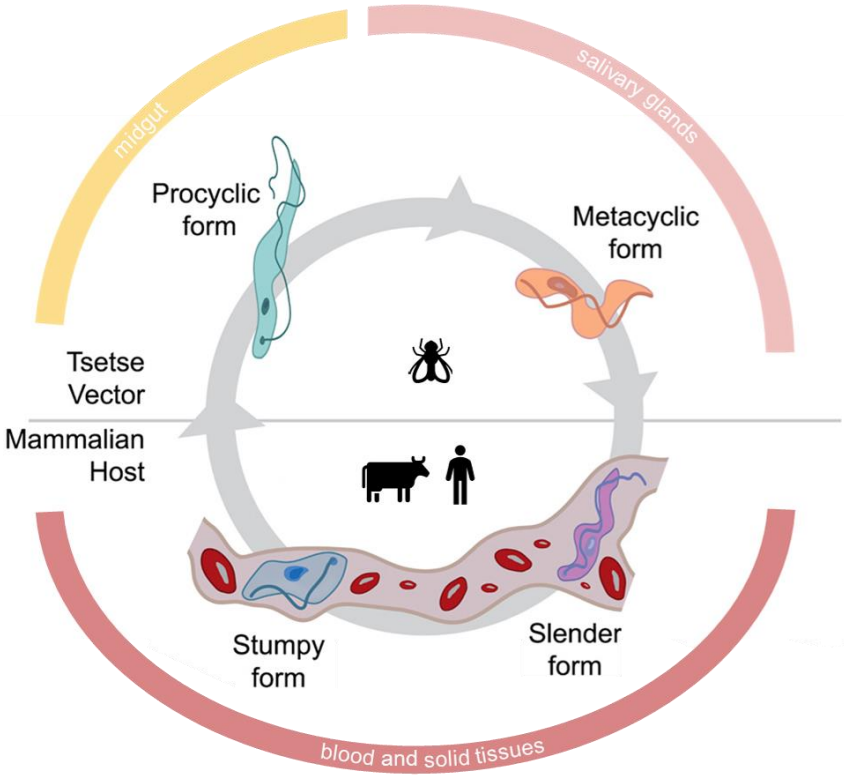


**Figure 2**. **Schematic representation of *T. brucei* life cycle.** *T. brucei* life cycle takes place in two hosts: the tsetse fly and a mammalian host. When a tsetse fly takes a bloodmeal, it injects metacyclic forms of the parasite in a susceptible mammalian host. These parasites then migrate to the bloodstream and into solid tissues and

differentiate into slender forms that cause an increase in parasitemia. Part of this population can then differentiate into cell cycle-arrested stumpy forms that are preadapted to survive in the tsetse fly. These stumpy forms are then taken up during another bloodmeal, restarting the transmission cycle. Adapted from 18.

### 1.1.2. Tissue tropism of *Trypanosoma brucei*

For a long time, *T. brucei* colonization was considered to be largely restricted to the circulatory and lymphatic systems, as well as the CNS in later stages of the disease. However, unlike other African trypanosomes (e.g., *T. congolense*) which occupy exclusively intravascular spaces, *T. brucei* colonizes the interstitial spaces of the infected host[11]. This process is modulated by tissue tropism, which can be defined as the ability of a pathogen to specifically infect a given tissue or organ. Tissue tropism can change as infection unfolds and it is mediated by host and pathogen factors[11,19,20]. Most organs in humans and animals have been recognized to sustain parasites since invasion of the bloodstream and lymph fluids allows for efficient dissemination through the body. For this reason, *T. brucei* is considered broadly tropic[11].

Tissue tropism may give rise to establishment of reservoirs. These reservoirs are normally prompted by tissue-specific features that can be exploited by the pathogen, like nutrient availability, immune response, ability to amplify transmission and permeability to drug treatments[11,20]. The skin[21–23], CNS[8,24,25], reproductive organs[26–28] and adipose tissue (AT)[18,29], are some of the characterized *T. brucei* reservoirs. This classification is based on criteria such as higher parasite load, relation to pathology and clinical signs[11].

#### 1.1.2.1. Skin tropism

The skin is a strategic site that may have an important role during parasite transmission. Indeed, a pool of proliferating parasites that stays in the skin following natural transmission has been identified in mice[22]. Another study detected viable trypanosomes in the dermis of mice up to 20 days after a tsetse fly bite[21]. Interestingly, a subset of parasites expressing protein associated with differentiation 1 (PAD1) stumpy-specific marker was present in different skin sections in variable proportions[21]. Capewell *et al.* also analyzed histological samples of human skin from undiagnosed individuals collected in a region of high HAT incidence, which revealed the presence of trypanosomes in some of them[21].

It has been proposed that transmissible forms of the parasite present in the skin can be taken up by the tsetse fly[21,22]. Moreover, the existence of asymptomatic carriers of trypanosomes without detectable parasitemia may increase the probability of tsetse fly infection during a blood meal. This is especially relevant since infected hosts present on average very low parasitemia, therefore it has been suggested that parasite uptake exclusively from the blood by a tsetse fly is insufficient to sustain transmission of African trypanosomiasis[30].

### 1.1.2.2. CNS tropism

HAT disease progression directly correlates to *T. brucei* invasion of the CNS. Neurological symptoms develop during this stage and are associated with severe pathology and high mortality. *T. brucei* invades on an early phase the meninges (meningeal stage) and later the brain parenchyma after crossing the blood-brain barrier (encephalitic stage), which culminates in coma and death[24]. Curiously, parasites were not able to survive and replicate when cultured in cerebrospinal fluid[24,25], which raises the question of whether the brain parenchyma is an environment where parasites can stay in a quiescent form.

The CNS is considered an 'immune privileged' site where several mechanisms protect vital structures from unwanted inflammation. Immune privilege could have adverse consequences during infection, limiting parasite clearance and creating a pool of parasites that can re-populate the blood [19,31]. Indeed, high numbers of dividing parasites were found permanently in the pia mater, from here they could re-invade the bloodstream[24,25].

Additionally, drugs used to treat first-stage HAT do not cross the blood-brain barrier and the number of drugs that successfully do is limited and associated with high toxicity which adds to the problem of eliminating *T. brucei*[4,8]. Lastly, neurological symptoms caused by CNS colonization such as disruption of sleep/wake cycles and apathy may allow the tsetse vector to have easier undisturbed blood meals on infected humans, thus promoting transmission events.

### 1.1.2.3. Reproductive organ tropism

Sexual transmission of *T. brucei* is recognized by WHO as a possible route of infection, though very rare[3]. There is only one case described in the literature where transmission through sexual contact seems likely to have occurred since the patient had never been to Africa[32]. Nonetheless, horizontal transmission via the sexual route was proven to exist in mice[26]. Healthy females who had been crossed with infected males harbored parasites in some of their reproductive organs, while showing no detectable parasitemia[26].

There are also reports of parasite tropism to male reproductive organs in murine models[26–28]. Experiments show that parasites accumulate mainly in the stroma of the epididymis[27], epididymal AT[27] and in the interstitial stroma of the testis, between the seminiferous tubules[28].

The testes also benefit from immune privilege, with several factors contributing to this status[33]. Like the blood-brain barrier protects the brain, the blood-testis barrier limits the passage of immune contents into the seminiferous tubules, shielding auto-antigenic germ cells from being recognized by the immune system[33]. In a similar way, the epididymis is protected by a barrier that also creates a safe environment for germ cell development, the blood-epididymis barrier[33].

Although parasites were not located in the immune privileged niches, they were accompanied by a marked inflammatory response that could lead to tissue damage and leaking of parasites to the semen[27]. This could allow trypanosome sexual transmission.

Finally, the blood-testis barrier might protect parasites from being efficiently cleared by trypanocidal drugs. Reactivation of infection occurred several days after sub-curative drug treatment and trypanosomes were detected in mice testis[28].

### 1.1.2.4. Adipose tissue tropism

One of the hallmarks of African trypanosomiasis in animals and humans is cachexia, a metabolic condition associated with extreme loss of muscle and fat[34]. Additionally, there is evidence suggesting that *T. brucei* can affect host metabolism during infection. In a study aimed at identifying disease metabolic markers, *T. brucei gambiense* infected individuals showed pronounced differences from controls in plasma lipid composition, with an overall decrease in lipid content but increased levels of triglycerides[35]. In mice, besides reduced levels of plasma lipids, analysis of urine composition also indicated that in later stages of the disease infected mice were in a ketotic state and lipids were used as an energy source by the host[36].

In 2016, Trindade *et al.* identified AT as a major reservoir for parasites in mice, often being the compartment with the highest parasite density during infection[18]. These parasites were infective as they were able to invade the bloodstream of naïve mice after injection of infected gonadal AT homogenates[18]. Parasites have been also found in subcutaneous AT[21] and electron microscopy revealed intricate interactions between skin-dwelling parasites and adipocytes in the connective tissue[22].

Identifying mediators of tropism is important to understand why parasites accumulate on certain sites and its effects on pathogenesis. AT tropism is partially mediated by cluster of differentiation 36 (CD36)[29]. CD36 was described as an important adhesion molecule for parasite extravasation specifically in AT[29]. Blocking CD36 resulted in a parasite decrease of 50% in the extravascular space of mice gonadal AT and a sharp decrease in parasite content in the blood, indicating that this molecule has a determinant role in disease progression[29].

How *T. brucei* benefits from AT remains to be elucidated. It is possible that drug treatment efficacy may be impaired in this tissue, as several drugs are hydrophilic and cannot diffuse properly in environments rich in lipids[37]. Another possibility is that nutrient availability in AT favors *T. brucei* persistence. This is especially relevant as adipose tissue forms (ATFs) of the parasite were shown to have a different metabolic profile from bloodstream forms (BSFs). Specifically, transcriptome analysis revealed upregulation of fatty acid metabolism genes in ATFs, suggesting an ability to metabolize these compounds as a carbon source[18]. Indeed, this was the case as ATFs, but not BSFs, were able to perform β-oxidation with labeled myristate[18].

Collectively, all the examples mentioned above lead us to speculate about the role of parasite reservoirs in transmission, disease progression and treatment relapse. Cases of long infection periods have been reported, the most impressive one being the case of a man who developed second stage Gambiense HAT at least 29 years after infection[38]. Likewise, cases where drug treatment is ineffective in eliminating all parasites within the host, are examples of situations where reservoirs might be involved[39].

Diagnostic methods are limited because they only detect positive cases of HAT when parasitemia is detectable or symptoms of second-stage disease have developed[40]. Serological testing also exists. However serologic positive patients without parasitemia and disease symptoms are not treated[40,41], which can further contribute to the existence of human trypanosome carriers. Consequently, understanding the dynamics of parasite tissue tropism and the ability to establish reservoirs in the host is of utmost importance for disease control.

## 1.2. Adipose tissue

The AT is a complex multi-depot organ (Figure 3) known traditionally to be the site of lipid storage, specialized in regulating and maintaining energy homeostasis[42,43]. It was once considered to be an inert tissue with the sole function of being an energy reservoir. But its role as a secretory and endocrine organ gained importance after the discovery of adipokines, a group of molecules responsible for regulating metabolism both locally and in other organs[43].

AT has a very heterogeneous cell composition. Adipose cells called adipocytes are the main cells in AT but they share their surroundings with the so-called stromal-vascular fraction composed of endothelial cells, fibroblasts, preadipocytes, stem cells and an array of immune cells, the main one being macrophages[42]. Adipocytes are responsible for storing triacylglycerols (TAGs) in the cytoplasmic lipid droplet. TAGs are classified as neutral lipids and represent a valuable energy source since their breakdown fuels the organism during fasting periods[43].

Based on differences in function, morphology and developmental origin, three types of AT have been identified: white adipose tissue (WAT), brown adipose tissue (BAT) and beige/brite adipose tissue.

White adipocytes are unilocular which means they possess a single large lipid droplet, and their main purpose is storing energy as TAGs. In a mature adipocyte, the lipid droplet can occupy up to 90% of the cell volume. In mammals, WAT is distributed across the body in several visceral and subcutaneous depots[43]. Visceral fat surrounds abdominal organs and is frequently associated with metabolic syndrome[43]. Subcutaneous WAT lies under the dermis. Its function in humans is believed to be protection against mechanical stress and heat loss[44]. Mice and humans differ in WAT distribution and some depots do not have direct homologues between both organisms[42]. There is also evidence that different depots of WAT differ in functional features like adipokine secretion and rate of lipolysis, which might make this classification broad and oversimplified[42].

BAT adipocytes are specialized in oxidizing substrates, so they possess multilocular lipid droplets and are very rich in mitochondria. Brown adipocytes can generate heat through a process called thermogenesis, which provides protection in cold environments[45]. This process requires uncoupling protein-1 (UCP-1), a unique proton transporter present in the inner mitochondrial membrane[45]. Only mammals have BAT, however, until recently, BAT depots in humans had been only described in newborns[42]. These depots would then regress with age. Nevertheless, recent imaging studies suggest that adults also possess BAT depots namely in the supraclavicular and spinal regions[42,45].

Beige adipocytes are considered an intermediate between WAT and BAT adipocytes since they possess characteristics of both cells. They can appear in WAT depots in response to certain stimuli but express an array of genes characteristic of brown adipocytes, including UCP-1 given them thermogenic capacity[46]. This process is called browning and it has been associated with protection against metabolic

complications[46]. Their morphology is also similar to BAT adipocytes, yet they do not share a common precursor cell[45].

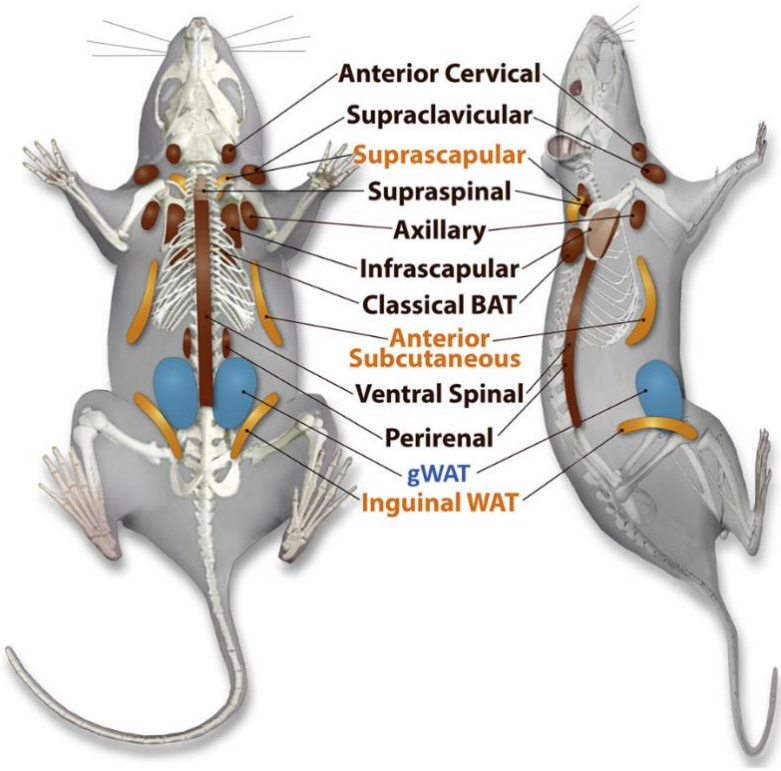


**Figure 3. Schematic representation of AT depots in mice.** WAT is represented in blue; BAT is represented in brown and WAT depots with beiging potential are represented in yellow. gWAT, gonadal white adipose tissue. Adapted from 47.

### 1.2.1. Lipolysis in adipocytes

TAGs exist in most eukaryotes[48]. In mammals, TAGs stored in WAT are the most important energy reserve. Besides adipocytes, other non-adipose cells can store and mobilize TAGs according to demand. However, lipolysis products in non-adipose cells are used in a cell autonomous manner and not systemically distributed to other tissues[49].

Within adipocytes, TAGs are kept inside the lipid droplet by a phospholipid monolayer coated with several proteins involved in lipid metabolism pathways such as lipid breakdown and synthesis and membrane-trafficking[50]. Besides serving as a deposit where TAGs are accumulated during times of energy abundance, lipid droplets give the cell a way to regulate their accessibility according to the need for substrates to produce energy or to synthesize important molecules, as well as protecting against lipotoxicity that could otherwise lead to cell dysfunction and death[50,51].

In periods of nutrient scarcity, stored lipids can be catabolized enzymatically into free fatty acids and glycerol through a pathway called 'neutral lipolysis'. Lipolysis consists in the sequential hydrolysis of TAGs by a cascade of three lipases that remove a non-esterified fatty acid (NEFA) at each stage. The final products are three NEFAs and one glycerol molecule which are then released in the blood. Insoluble NEFAs are transported to tissues associated to a carrier protein, albumin[52]. On arriving to NEFA-requiring tissues, β-oxidation takes place. Glycerol is transported to the liver where it can be converted to glucose[52].

#### 1.2.1.1. Intracellular regulation of lipolysis

Neutral lipolysis is initiated by adipose triglyceride lipase (ATGL) present in the adipocyte cytoplasm but also associated with the lipid droplet and responsible for hydrolyzing TAG to form diacylglycerol (DAG)[53] (Figure 4). Knockdown of this enzyme in mice led to accumulation of TAGs in non-adipose tissues as well as enlargement of fat depots, which established ATGL activity as a rate-limiting step in lipolysis[54].

The hydrolytic activity of ATGL is regulated by the activator comparative gene identification-58 (CGI-58), via protein-protein interactions, and by the inhibitor G0/G1 switch protein 2 (G0S2), which binds directly to ATGL independently of CGI-58[55]. ATGL activity is also affected indirectly by perilipin-1 (PLIN1) and fatty acid-binding proteins (FABPs) since these interact with CGI-58[51,55]. PLIN1 is the most abundant protein present in the lipid droplet monolayer, besides forming a barrier that protects TAG from lipases it is also responsible for coordinating lipase activity during lipolysis[50,56]. Under basal conditions (no stimulation by hormones), CGI-58 is sequestered by PLIN1, making it unavailable to bind to ATGL[55].

FABPs are a family of proteins that bind NEFAs with high affinity and FABP4 specifically is involved in adipocyte intracellular trafficking[56]. Experiments showed that FABP4 leads to increased activity of ATGL in the presence of CGI-58, but the mechanism by which these two proteins interact is still unknown[55].

The next enzyme in the cascade is hormone-sensitive lipase (HSL) which hydrolyzes DAGs into monoacylglycerols (MAG) (Figure 4). HSL presents activity on a wider number of substrates: TAGs, DAGs, MAGs, cholesteryl esters, retinyl esters and short-chain carbonic acid esters[51]. For some time, this enzyme was presumed to start the lipolytic pathway. However, the fact that HSL-null mice were lean[57], accumulated DAG and not TAG[58] and the discovery of ATGL[53], established hydrolysis of DAGs as the enzyme's main metabolic role[51,58]. Like ATGL, HSL is present in the cytoplasm and moves to the lipid droplet upon activation. Control of HSL activity is made by hormones, which will be discussed later in this chapter.

Release of the last NEFA and glycerol is mediated by the cytoplasmic monoacylglycerol lipase (MGL) (Figure 4). MGL has a high affinity for MAG, but its loss can be partially compensated by HSL[59]. Regulation of MGL is still unclear, nevertheless it seems that this enzyme is constitutively expressed[56,59].

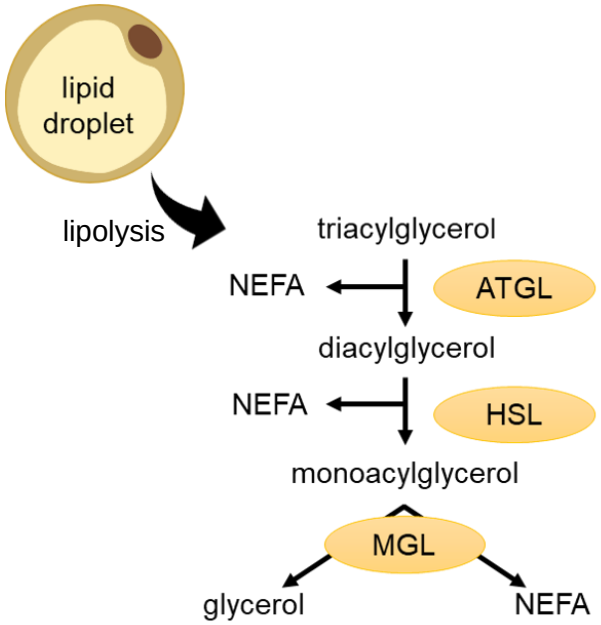


**Figure 4. Diagram of the lipolytic pathway.** Mobilization of triacylglycerols occurs through lipolysis and is mediated by three enzymes in a sequential manner. The final products are three NEFAs and one glycerol. ATGL, adipose triglyceride lipase; HSL, hormone-sensitive lipase; MGL, monoacylglycerol lipase; NEFA, non-esterified fatty acid.

### 1.2.1.2. Activators of lipolysis

Different cues can start the process of TAG mobilization and breakdown and it normally involves a crosstalk between adipocytes and other cells. These cues include hormonal, inflammatory and microbial signals.

#### 1.2.1.2.1. Hormones

The classic and best characterized pathway of lipolysis is hormonally regulated through the action of catecholamines, adrenalin and noradrenalin (Figure 5).

Under stimulated conditions, catecholamines bind to β-adrenergic receptors coupled with G-proteins, on the plasma membrane of adipocytes[56]. This leads to the activation of adenylate cyclase (AC) that converts adenosine triphosphate (ATP) to cyclic adenosine monophosphate (cAMP). The increase

in cAMP levels inside the cell activates protein kinase A (PKA) that phosphorylates PLIN1 and HSL[56]. PLIN1 phosphorylation mediates the release of CGI-58, which is now available to bind ATGL. CGI-58 has no hydrolytic activity but increases ATGL activity up to 20-fold[55,56]. Besides its role in ATGL activation, phosphorylated PLIN1 also translocates to the cytosol, making the lipid droplet surface more accessible for lipase attack[59]. After phosphorylation, HSL moves from the cytosol to the lipid droplet, beginning the hydrolysis of DAGs[59]. Association of NEFA-bound FABP4 to phosphorylated HSL seems to be another regulation step on the pathway since without FABP4 lipolysis decreases[60].

Other hormones like growth hormone, glucocorticoids and thyroid-stimulating hormone also act through the cAMP-dependent pathway to stimulate lipolysis. This can be done directly by specific receptors or indirectly by remodeling the lipolytic pathway[59].

Natriuretic peptides (atrial and brain) bind natriuretic peptide receptor type A (NPR-A), with intrinsic guanylate cyclase activity, and induce lipolysis by a pathway that leads to an increase of intracellular cyclic guanosine monophosphate (cGMP) levels with activation of protein kinase G (PKG)[59] (Figure 5). PKG also phosphorylates HSL and PLIN1. These molecules are important lipolysis stimulators, especially during physical activity.

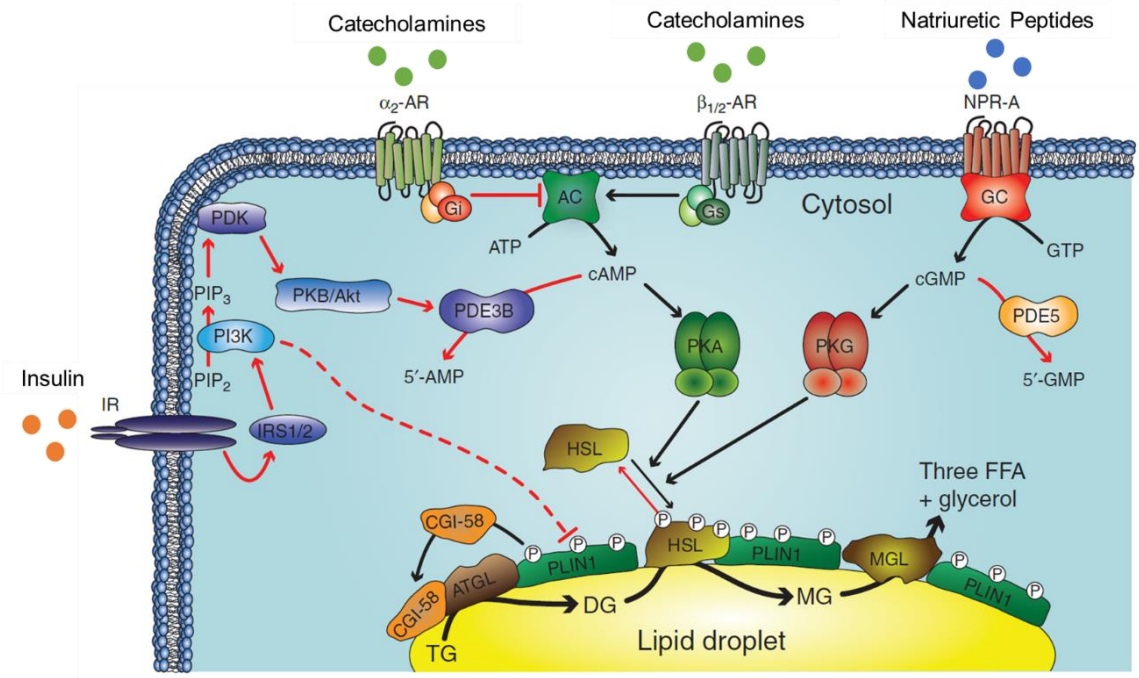


**Figure 5. Overview of the major hormonal lipolytic signaling pathways.** Black lines indicate pro-lipolytic pathways while red lines indicate anti-lipolytic pathways. $\alpha_2$-AR, $\alpha_2$-adrenergic receptor; AC, adenylate cyclase; TG, triglyceride; ATGL, adipose triglyceride lipase; $\beta_{1/2}$-AR, $\beta_1$- and $\beta_2$-adrenergic receptors; CGI-58, comparative gene identification-58; DG, diacylglycerol; FFA, free fatty acid; GC, guanylate cyclase; HSL, hormone-sensitive lipase; IR, insulin receptor; IRS1/2, IR substrates 1 and 2; MG, monoacylglycerol; MGL, monoacylglycerol lipase; NPR-A, natriuretic peptide receptor type A; PDE3B, phosphodiesterase 3B; PDK, phosphoinositide-dependent kinase; PI3K, phosphoinositol-3-kinase; PKA, protein kinase A; PLIN1, perilipin 1. Adapted from 59.

#### 1.2.1.2.2. Cytokines

Lipolysis can also be positively regulated locally by paracrine and autocrine effectors, like cytokines and adipokines.

Tumor necrosis factor-alpha (TNF-α) is a pro-inflammatory cytokine mainly produced by macrophages in the AT but also adipocytes[56]. Originally, it was named 'cachectin' due to its association with cachexia disorders. It acts both by stimulating lipolysis and inhibiting lipogenesis[59]. Binding to TNF receptor 1 leads to the stimulation of lipolysis through multiple non-canonical pathways[61]. This is mediated by the downstream activation of other kinases involved in the lipolytic response, including mitogen-activated protein kinases (MAPK) namely extracellular-signal-regulated kinase (ERK) 1/2 (p42/44) and c-Jun N-terminal kinase (JNK)[61,62].

TNF-α inhibits anti-lipolytic signaling of insulin by phosphorylation of insulin receptors and its signaling molecules (insulin receptor substrate-1), and by intervening in insulin-mediated cAMP hydrolysis[63]. This last factor leads to an indirect increase of phosphorylated PLIN1. While catecholamine-stimulated lipolysis is initiated within minutes, TNF-α takes between 6-12h to activate lipolysis[64]. Due to its delayed effect in stimulating lipolysis, transcriptional regulation is probably also involved[64].

Interleukin-6 (IL-6) is also a pro-inflammatory cytokine expressed in WAT adipocytes[56]. IL-6 increases both basal and PKA-activated lipolysis[60] and reduces insulin antilipolytic signaling[63].

#### 1.2.1.2.3. Microbial factors

Adipocytes also express pathogen recognition receptors (PRRs) including most Toll-like receptors (TLRs) and nucleotide-binding oligomerization domain containing proteins (NOD) 1/2 which allow for the recognition of pathogen-associated molecular patterns (PAMPs)[65]. Interestingly, the gut microbiota influences AT metabolism which indicates that adipocytes can respond to secreted bacterial metabolites[66]. Furthermore, the ability of bacterial factors like lipopolysaccharides (LPS) or peptidoglycan to induce lipolysis has been demonstrated[67,68].

### 1.2.1.3. Inhibitors of lipolysis

The classic and most important repressor of lipolysis is insulin (Figure 5). Binding of the hormone to insulin receptors leads to activation of phosphoinositol-3-kinase (PI3K) signaling, which activates the enzyme phosphodiesterase 3B (PDE3B)[59]. PDE3B promotes cAMP hydrolyzation and decreases PKA activity, reducing phosphorylation and activation of PLIN1 and HSL[59].

Catecholamines can also have an antilipolytic effect (Figure 5). This is mediated by binding to $\alpha_2$-adrenergic receptors, which inhibit AC activity and block production of cAMP[69]. Inhibition or stimulation of lipolysis depends on the affinity of the hormones to the receptors and the receptor's enrichment in the adipocyte plasma membrane[69].

Neuropeptides and other metabolites produced by the adipocytes or cells in the stromal vascular fraction (adiponectin, adenosine and prostaglandins) also have an antilipolytic effect[56,63].

### 1.2.2. Lipophagy in adipocytes

Besides neutral lipolysis, breakdown of lipids can also occur via lipophagy. Autophagy is a catabolic pathway through which cytosolic components are degraded in the lysosome. During lipophagy, small lipid droplets or portions of big lipid droplets can be degraded. Degradation of TAGs associated to lysosomes is called 'acid lipolysis'. Parts of lipid droplets are engulfed by a lipoautophagosomes that then fuse with a lysosome to form an autolysosome. Inside autolysosomes, TAGs are degraded by lysosomal acid lipase (LAL). LAL can act on several substrates: TAGs, DAGs, cholesteryl esters and retinyl esters[51]. The products of its activity are NEFAs, unesterified cholesterol and retinol[51]. Regulation of LAL is made mainly at the transcription level[51].

## 1.3. Adipose tissue as a site of infection

Many microorganisms can invade and establish in AT. Here, they can alter many aspects of the tissue metabolism, like cytokine production, adipocyte metabolic pathways, fat distribution, among others. Frequently, favoring a pro-inflammatory response and dysregulating energy homeostasis.

### 1.3.1. Viral pathogens

Viruses are obligatory intracellular infectious agents since they need a host living cell to be able to replicate. Inside the cell, they hijack the biosynthetic machinery, subverting host cellular processes in surprising ways.

For example, infection by human Adenovirus 36 is frequently associated with obesity, since the virus can induce adipogenesis leading to expansion of fat depots[70]. *In vitro* studies demonstrated that the Adenovirus 36 favors replication and differentiation of preadipocytes into adipocytes and lipid accumulation in human and murine adipocytes, having an impact on gene expression of several adipocyte enzymes and transcription factors[70,71].

Patients undergoing human immunodeficiency virus 1 (HIV-1) antiretroviral therapies experience HIV/antiretroviral therapy-associated lipodystrophy syndrome (HALS), characterized by a redistribution of fat, especially subcutaneous[72]. The ability of HIV-1 to infect adipocytes is controversial, since the adipocytes express the co-receptors for viral entry, but apparently not in a sufficient number to establish infection[73]. Nonetheless, infected immune cells (CD4+ T cells and macrophages, mainly) seem to create a reservoir for HIV-1 in AT[74]. Untreated infected patients also experience some milder alterations in AT, including loss of weight and fat mass[75]. Indeed, the circulation of viral proteins in AT and their effect in peroxisome proliferator-activated receptor γ (PPARγ), an adipocyte master transcription factor and regulator of adipogenesis, has been described and it could contribute to dysregulation of adipocyte metabolism[75,76]. Studies in a murine model revealed that HIV's viral protein R (Vpr) induced co-repression of PPARγ and co-activation of the glucocorticoid receptor[76]. Mice showed enhanced whole-body lipolysis, hyperglycemia and hypertriglycemia[76]. Additionally, to further understand the effect of Vpr on adipocytes, 3T3-L1 Vpr-expressing adipocytes showed that the viral protein blocks differentiation of preadipocytes and induces lipolysis in mature adipocytes[76].

### 1.3.2. Bacterial pathogens

Intracellular bacteria *Rickettsia prowazekii* (*R. prowazekii*) is responsible for causing Brill-Zinsser disease, a recrudescent form of epidemic typhus. This relapse occurs frequently many years after

primary infection, suggesting that the bacterium remains latent in some patients[77]. Bechah *et al*. detected *R. prowazekii* DNA in AT of mice 4 months after recovery from the primary infection, while there was no detection in other tissues. Furthermore, bacteria recovered from homogenized AT were cultured and viable[78].

Relapses of Q fever after treatment have been also described in some patients. *Coxiella burnetii* (*C. burnetii*), the causative agent of Q fever and another intracellular bacterium, was also shown to persist in AT. In this study, the transcriptional profile of infected 3T3-L1 adipocytes was analyzed. *C. burnetii* induced a transcriptional inflammatory signature which included gene networks around proinflammatory cytokines (IL-6 and TNF-α), chemokines, transcription factor nuclear factor kappa light chain enhancer of activated B cells (NF-κB) and TLR-2. This response could be involved in latent infection of AT[79].

*Mycobacterium tuberculosis* (*M. tuberculosis*) infects primarily alveolar macrophages where it can stay quiescent for long periods without clinical signs, a state called latent tuberculosis. However, the bacillus can also exist in extrapulmonary sites. In 2006, Neyrolles *et al.* showed that AT could be a niche that allowed for *M. tuberculosis* persistence without replication. The mycobacteria were able to enter 3T3-L1 mouse adipocytes as well as primary human adipocytes *in vitro* and accumulated many cytoplasmic lipid droplets[80]. Additionally, foamy macrophages, infected macrophages that accumulate several cytoplasmic lipid droplets, seem to provide dormant *M. tuberculosis* a source of lipids. Using an *in vitro* model of foamy macrophages, Daniel *et al.* were able to demonstrate that *M. tuberculosis* can import host fatty acids and incorporate them into their own intracellular lipid droplets, during the synthesis of TAGs. *M. tuberculosis* also possesses their own lipases. For example, LipY, which belongs to the hormone-sensitive lipase family, can hydrolyze host and bacterial TAGs[81,82].

### 1.3.3. Protozoan pathogens

Other kinetoplastids also find in adipocytes a place where they can persist. It's well-established that *T. cruzi* uses AT as a reservoir during Chagas disease chronic phase. Both experiments in mice and biopsies from human patients showed evidence of *T. cruzi* persistence in AT[83,84].

*T. cruzi* is able to infect WAT and BAT in mice[85]. Infection by this intracellular parasite deeply affects different factors of adipocyte metabolism. Fifteen days after WAT infection, there was 25% loss of lipids accompanied by a significant reduction in adipocyte size[85]. Western blot analysis also revealed that HSL expression was increased relative to the controls, suggesting an increase in lipolysis[85]. Indeed, electron micrographs showed that parasites are frequently close to the surface of WAT lipid droplets[84].

Expression of a number of cytokines and adipokines was also affected including downregulation of adiponectin and overexpression of TNF-α, favoring a proinflammatory effect[84–86].

The mouse AT is also a major site of sequestration of the malaria-causing parasite, *Plasmodium berghei* (*P. berghei*)[87]. The same had been previously reported in the night monkey during infection with *Plasmodium falciparum*[88]. When in the blood, *Plasmodium* spp. infect red blood cells (RBCs). Sequestration refers to the ability of infected RBCs to adhere to the endothelial cells of blood vessels in several tissues and is normally associated to pathogenesis[37,87]. Interestingly, CD36 also appears to be an important mediator of sequestration of *P. berghei* in blood vessels of AT[87].

The metabolic and functional properties of adipocytes can be modulated by pathogens to fuel their proliferation and favor persistence. Different pathogens achieve this modulation with distinct strategies. On one hand, this modulation can be done by changing inflammatory or hormonal cues in the AT milieu to which adipocytes are sensitive. On the other hand, this can be achieved by directly interacting with receptors on the adipocyte's surface (or cytoplasm in the case of intracellular pathogens) or by direct sequestration of metabolites.

## 1.4. Ongoing studies of lipolysis in *T. brucei* infection

During *T. brucei* infection, the host undergoes a progressive loss of adipocyte volume that correlates with an increase in adipocyte lipolysis (Machado *et al*, unpublished data). Specifically, between days 6 and 10 post-infection an increase in NEFA and glycerol release is observed in the gonadal white adipose tissue (gWAT) and other WAT depots. This increase in AT lipolysis is predominantly ATGL-dependent and results in a ≈ 75% reduction of total gWAT weight and adipocyte volume.

Additionally, vast numbers of *T. brucei* parasites are observed interacting with adipocytes of the infected host. This process is accompanied by a progressive influx of immune cells[89]. The question of whether the observed increase in AT lipolysis is mediated by immune cues, hormonal signaling or a direct adipocyte-*T. brucei* interaction remains to be elucidated.

In this work we explored the potential role for direct adipocyte-*T. brucei* interactions in the modulation of adipocyte metabolism.

## 1.5. Aims of this study

We hypothesized that interaction between *T. brucei* and adipocytes would result in an increase in adipocyte lipolysis. The main goal of this thesis is to investigate the *in vitro* influence of *T. brucei* on:

1. Release of lipolytic products (NEFAs and glycerol) by adipocytes.
2. Expression and activation levels of lipases.

# 2. Materials and Methods

## 2.1. Trypanosome strains and culture

Two trypanosome strains were used: the monomorphic bloodstream form *T. brucei brucei* Lister 427 and the pleomorphic bloodstream form *T. brucei brucei* AnTat1.1 90:13, derived from the EATRO1125 strain. Both strains were maintained in HMI-11 medium and incubated at 37ºC in 5% $CO_2$.

## 2.2. Trypanosome lysates

Lister 427 trypanosomes were cultured as described above, harvested and centrifuged at 1872 x g for 15 minutes at 4ºC. The parasite pellet was then washed in sterile phosphate-buffered saline (PBS) and the suspension centrifuged at 1872 x g for 15 minutes at 4ºC. For further use in co-culture experiments, the parasites were resuspended in low-glucose (1 g/L) DMEM (Gibco, Thermo Fisher Scientific Inc., USA) at $5x10^8$ trypanosomes/mL and kept in ice. Lysis was achieved by doing 3 snap freeze-thaw cycles in liquid nitrogen and by forcing the suspension through a 29 Gauge insulin syringe between cycles. To remove clumps of cell debris, a final centrifugation at 1872 x g for 1 minute at 4ºC was performed. The supernatant was then collected, divided into aliquots, snap-frozen in liquid nitrogen and stored at -80ºC.

To confirm efficacy of the trypanosome lysate protocol, samples were resolved by sodium dodecyl sulphate polyacrylamide gel electrophoresis (SDS-PAGE) as described below and the gel subjected to Coomassie blue protein staining. Briefly, the gel was incubated with Coomassie blue staining solution[90] for 20 minutes under gentle agitation at room temperature. Subsequently, several washes with replenishing of the destaining solution (40% methanol and 10% glacial acetic acid) were performed at room temperature until background of the gel was fully destained.

## 2.3. Maintenance and differentiation of 3T3-L1 adipocyte culture

The 3T3-L1 mouse embryonic fibroblast commercial cell line (CL173™; American Type Culture Collection, USA) was used as *in vitro* model for adipocytes. 3T3-L1 preadipocytes were cultured with high-glucose (4.5 g/L) Dulbecco's modified Eagle's medium (DMEM; Gibco, Thermo Fisher Scientific Inc., USA) supplemented with 10% iron-supplemented heat-inactivated bovine calf serum (BCS; Sigma-Aldrich, Merk, Germany) and kept at 37ºC in 5% $CO_2$. The media was changed every 2 days,

except when seeding cryopreserved cells in which case it was changed after 24 hours to remove cell debris.

When the preadipocyte culture reached 70-80% confluency, it was dissociated with 0.25% trypsin (Sigma-Aldrich, Merk, Germany). For further experiments, preadipocytes were resuspended at $5x10^4$ cells/mL in high-glucose DMEM supplemented with 10% BCS, seeded in 12-well plates (1 mL/well), and incubated for 4 days until reaching 100% confluency.

For terminal differentiation, cells were treated for 48h with a differentiation cocktail consisting of 1 μg/mL insulin (Insulin Solution Human; Sigma-Aldrich, Merk, Germany), 0.5 mM 3-isobutyl-1-methylxanthine (IBMX; Sigma-Aldrich, Merk, Germany), and 1 μM dexamethasone (Sigma-Aldrich, Merk, Germany) which was added to high-glucose DMEM supplemented with 10% heat-inactivated fetal bovine serum (FBS; Gibco, Thermo Fisher Scientific Inc., USA). This media was replaced by high-glucose DMEM supplemented with 10% heat-inactivated FBS, 1 μg/mL insulin, and incubated for further 48h. Afterwards, media was replaced every 48 hours with high-glucose DMEM supplemented with 10% heat-inactivated FBS until enough TAG accumulation was observed. When necessary, a second round of differentiation was performed.

After differentiation, the media should be changed every 2 days using high-glucose DMEM supplemented with 10% heat-inactivated FBS.

## 2.4. Co-cultures

### 2.4.1. 3T3-L1 and trypanosome co-culture

Parasites were cultured as described above, centrifuged at 827 x g for 15 minutes, harvested and resuspended to the desired inoculum in low-glucose DMEM supplemented with 10% heat-inactivated FBS.

Adipocytes previously seeded in 12-well plates were inoculated with *T. brucei* and incubated for 6h or 24h, according to the experimental setup. Plates were kept at 37ºC in 5% $CO_2$ during incubation periods. Control groups included adipocyte cultures with no parasites (negative control). Each experimental and control group was done in biological triplicates.

For each time-point different plates were used for lipolytic product quantification, RNA extraction, protein extraction and assessment of parasite growth. For quantification of lipolytic products, two additional series of incubations were carried out and media collected. Cells were incubated for 2 hours in low-glucose DMEM with 5% (w/v) fatty acid-free bovine serum albumin (BSA; Sigma-Aldrich, Merk, Germany) and later incubated for 1h with low-glucose DMEM with 5% (w/v) fatty acid-free BSA and 10 μM forskolin (Abcam, United Kingdom). For RNA and protein extraction, cells were resuspended in the respective lysis solutions as described in the sections below. For assessment of parasite growth, live trypanosomes were counted using a haemocytometer.

Inhibition of ATGL was accomplished by adding 50 μM atglistatin (Sigma-Aldrich, Merk, Germany) to all incubation medias mentioned above. To conditions with non-inhibited ATGL (control), the corresponding volume of the vehicle, dimethyl sulfoxide (DMSO), was added.

To study the effect of direct physical contact between adipocytes and parasites a transwell system (12 mm Transwell® with 0.4 μm pore polycarbonate membrane insert; Costar, Corning Inc., USA) was used. Adipocytes were cultured on the bottom as mentioned while parasites were inoculated on the overlying transwell insert. Lipolysis measurements were performed as described above, in the absence of the transwell insert.

### 2.4.2. Adipose tissue explant and trypanosome co-culture

Male C57BL/6J mice from Charles River Laboratories International were euthanized by $CO_2$ narcosis and gWAT was collected. Harvested tissue was rinsed in high-glucose DMEM, cut in ~20-30 mg fragments, placed in 96-well plates (1 explant/well) and incubated according to the experimental set up in low-glucose DMEM supplemented with 10% heat-inactivated FBS at 37ºC in 5% $CO_2$. gWAT explants with no parasites were used as the control group (negative control). Lipolysis measurements were performed as described above and normalized to explant protein content.

## 2.5. RNA protocols

### 2.5.1. RNA extraction from 3T3-L1 co-culture

After incubation, media was removed and the 3T3-L1 adipocyte monolayer resuspended in TRIzol® Reagent (Invitrogen, Thermo Fisher Scientific Inc., USA) for total RNA extraction. Extraction was performed with 500 μl of TRIzol according to the manufacturer's instructions with some modifications. All centrifugations were made at 4ºC. Since samples had a high-fat content, an initial centrifugation at 12000 x g for 5 minutes was done to clarify the supernatant. Adding chloroform separated the clarified supernatant in two phases after centrifugation at 12000 x g for 15 minutes. The top aqueous phase containing the RNA was collected and the RNA precipitated by adding isopropanol with 5 μg/sample GlycoBlue™ Coprecipitant (Invitrogen, Thermo Fisher Scientific Inc., USA), incubating for 10 minutes on ice and centrifuging for 10 minutes at 12000 x g. Pellet was washed twice with 75% ethanol, centrifuged for 5 minutes at 7600 x g between each washing step, and air-dried for 10 minutes. Finally, the precipitated RNA was resuspended in 21.5 μl of RNase-free dd$H_2O$ and incubated for 15 minutes at 55ºC.

To quantify RNA and assess quality, absorbance was measured at 260 nm and 280 nm using NanoDrop 2000 Spectrophotometer (Thermo Fisher Scientific Inc., USA).

### 2.5.2. Reverse transcription polymerase chain reaction (RT-PCR)

Complementary DNA (cDNA) was synthesized from 1-5 µg of total RNA with the NZY Reverse Transcriptase (NZYTech, Portugal) using random hexamer primers according to the manufacturer's instructions. Briefly, 1 µg of total RNA was mixed with 1 µl 10 mM dNTPs, 1 µl random hexamer primers, 200 U reverse transcriptase and 2 µl 10X reaction buffer in a total volume of 20 µl.

RT-PCR was carried out in the T100™ Thermal Cycler (Bio-Rad Laboratories, USA) under the following protocol: 25ºC for 10 minutes, 50ºC for 50 minutes, and 85ºC for 5 minutes. cDNA samples were then diluted by adding 60 µl RNase-free dd$H_2O$.

### 2.5.3. Quantitative polymerase chain reaction (qPCR)

qPCR was carried out using 4 µl of cDNA as template, 5 µl of Power SYBR® Green PCR master mix (Applied Biosystems, Thermo Fisher Scientific Inc., USA) and 0.5 µl of each gene-specific primer (Sigma-Aldrich, Merk, Germany). The sequences of the primers used are listed in Table 1.

**Table 1.** Sequences of SYBR Green primers.

| Gene | Organism | Primer sequence (5'-3') |
|---|---|---|
| *Pnpla2* (ATGL) | Mouse | Fw: CAACGCCACTCACATCTACGG<br>Rv: TCACCAGGTTGAAGGAGGGAT |
| *Gapdh* | | Fw: AGGTCGGTGTGAACGGATTTG<br>Rv: AGGTCGGTGTGAACGGATTTG |
| *Lipa* (LAL) | | Fw: TGCCCACGGGAACTGTATC<br>Rv: ATCCCCAGCGCATGATTATCT |
| *Lipe* (HSL) | | Fw: GGCTCACAGTTACCATCTCACC<br>Rv: GAGTACCTTGCTGTCCTGTCC |
| *β-actin* | | Fw: AGAGGGAAATCGTGCGTGAC<br>Rv: CAATAGTGATGACCTGGCCGT |
| *18S rRNA* | | Fw: GGACCAGAGCGAAAGCATTTGCC<br>Rv: TCAATCTCGGGTGGCTGAACGC |
| *Mgll* (MGL) | | Fw: CGGACTTCCAAGTTTTTGTCAGA<br>Rv: GCAGCCACTAGGATGGAGATG |
| *Fasn* (FAS) | | Fw: GGAGGTGGTGATAGCCGGTAT<br>Rv: TGGGTAATCCATAGAGCCCAG |
| *Hprt* | | Fw: TCAGTCAACGGGGGACATAAA<br>Rv: GGGGCTGTACTGCTTAACCAG |

*Pnpla2* (patatin-like phospholipase domain-containing protein 2), *Gapdh* (glyceraldehyde 3-phosphate dehydrogenase), *Fasn* (fatty acid synthase), *Hprt* (hypoxanthine-guanine phosphoribosyl transferase). Fw, forward primer. Rv, reverse primer.

Amplification was performed on the Applied Biosystems QuantStudio™ 5 Real-Time PCR system (Thermo Fisher Scientific Inc., USA) under the following protocol: 2 minutes at 50ºC, 10 minutes at 95ºC and 40 cycles (95ºC for 15 seconds, 55ºC for 15 seconds, 72ºC for 30 seconds). This was followed by a melt curve analysis to assess amplicon specificity: 15 seconds at 95ºC, 1 minute at 60ºC and 15 seconds at 95ºC. RNase-free dd$H_2O$ was used as negative control.

mRNA expression levels were determined based on the ΔΔCt method[91]. Data is presented as fold-change relative to *Gapdh*.

## 2.6. Protein protocols

### 2.6.1. Protein extraction from 3T3-L1 co-culture

Total protein was extracted using radioimmunoprecipitation assay (RIPA) lysis buffer[92] supplemented with 1% (v/v) phosphatase inhibitor cocktail 3 (Sigma-Aldrich, Merk, Germany) and protease inhibitor cocktail (Sigma-Aldrich, Merk, Germany). During extraction, the plate was kept on ice. After incubation, media was removed and 3T3-L1 cells were washed twice with cold PBS. After washing, ~400 µl of cold RIPA buffer was added to each well and left for 5 minutes. Cells were scraped from the bottom, gently resuspended, and transferred to a centrifuge tube. The supernatant was collected after centrifugation at 14,000 x g for 15 minutes at 4°C.

Total protein concentration was determined using the Pierce™ BCA Protein Assay Kit (Thermo Fisher Scientific Inc., USA), an adaptation of the traditional bicinchoninic acid (BCA) protein assay.

### 2.6.2. Protein extraction from adipose tissue explant co-culture

Total protein was extracted from snap-frozen gWAT explants. Tissue explants were homogenized with 1 mm zirconia/silica beads (BioSpec Products, USA) in a bead beater in 1 mL RIPA buffer[92]. To remove cell debris, the homogenate was centrifuged at 10,000 x g for 6 minutes and the supernatant transferred to a clean tube.

Total protein concentration was determined using the Pierce™ BCA Protein Assay Kit (Thermo Fisher Scientific Inc., USA).

### 2.6.3. SDS-PAGE and western blot

Protein samples were resolved by SDS-PAGE using the Any kD™ Mini-PROTEAN® TGX™ precast protein gel (Bio-Rad Laboratories, USA). Before loading, samples with equal amounts of protein were mixed with 6X Laemmli sample buffer in a total volume of 25 µl and heated at 95°C for 5 minutes.

Precision Plus Protein Dual Xtra Standards (Bio-Rad Laboratories, USA) was used as protein molecular weight marker. The SDS-PAGE gel was run at 140 V for 1 hour with 1X Tris-Glycine-SDS (TGS) running buffer (Bio-Rad Laboratories, USA) previously kept at 4°C.

The proteins were then transferred from the SDS-PAGE gel to a polyvinylidene fluoride membrane (PVDF; Invitrogen, Thermo Fisher Scientific Inc., USA) using the iBlot Dry Blotting System (Invitrogen, Thermo Fisher Scientific Inc., USA) according to the recommended voltage program for PVDF membranes (20 V for 7 minutes). To confirm transfer success the membrane was subsequently stained with Ponceau S for 5 minutes at room temperature. After several washes with $ddH_2O$ to remove the dye, the PVDF membrane was incubated in 20 mL of blocking buffer consisting of Tris-buffered saline, 0.1% Tween 20 (TBST) containing 5% (w/v) BSA for 1 hour at room temperature with gentle agitation.

The primary antibody was diluted according to the manufacturer's instructions (Table 2) in 5 mL of blocking buffer and incubated with the blot overnight at 4°C with gentle agitation. After washing the blot 3 times with TBST for 5 minutes, it was further incubated for 1 hour at room temperature with horseradish peroxidase-linked secondary antibody, anti-rabbit IgG (Amersham, GE Healthcare, USA) diluted 1:10000 in 10 mL of blocking buffer. The membrane was washed in TBST as mentioned before and incubated in enhanced chemiluminescence (ECL) substrate solution (Western Lightning Plus-ECL; PerkinElmer, USA). Chemiluminescence signal was detected with Amersham Imager 680 (GE Healthcare, USA).

**Table 2.** List of antibodies used in western blotting.

| Antibody | Dilution | Protein size | Host | Type | Source |
|---|---|---|---|---|---|
| anti-ATGL | 1:1000 | 54 kDa | Rabbit | Monoclonal | Cell Signaling Technologies, USA |
| anti-Phospho-HSL (Ser563) | | 81,83 kDa | | | |
| anti-β-actin | | 45 kDa | | | |

β-actin was used as loading control for expression normalization. Detection of this protein was always done after stripping the membrane previously incubated with the primary antibody against the protein of interest. For stripping, the membrane was incubated 3 times with mild stripping buffer (Table 3) for 10 minutes at room temperature. After washing the membrane twice with PBS for 10 minutes and twice with TBST for 5 minutes, it was ready for blocking and the protocol resumed as mentioned. Results were analyzed using ImageJ software (National Institutes of Health, USA).

**Table 3.** Western blot membrane stripping buffer.

| Mild stripping buffer |
|---|
| 15 g glycine |
| 1 g SDS |
| 10 mL Tween 20 |
| dd$H_2O$ up to 1 L |
| Adjust pH to 2.2 with HCl |

## 2.7. Lipolytic product quantification

Quantification of NEFA and glycerol released in the incubation media was performed under two different conditions: basal and stimulated. For the basal condition, low-glucose DMEM with 5% (w/v) fatty acid-free BSA was incubated with the cell culture for 2h. The stimulated condition used the same media described above with 10 μM forskolin and was incubated with the cell culture for 1h, to assess adipocyte responsiveness.

Glycerol and NEFA were quantified using the Glycerol Assay Kit (Sigma-Aldrich, Merk, Germany) and the Free Fatty Acid Quantification Kit (Sigma-Aldrich, Merk, Germany), respectively, according to the manufacturer's instructions for colorimetric detection. Absorbance was measured in the TECAN Infinite M200 microplate reader (Tecan Trading, Switzerland). Data are expressed as release rate per well (3T3-L1 co-culture) or per mg of protein (explant co-culture).

## 2.8. Data analysis

GraphPad Prism version 8.0.0 (GraphPad Software Inc., USA) was used for data presentation and statistical analysis. Data are presented as mean ± SEM (standard error of mean). One-way analysis of variance (ANOVA) with Sidak post hoc test was performed to compare experimental groups. Differences were considered statistically significant when $p<0.05$.

# 3. Results

## 3.1. 3T3-L1 adipocyte co-culture can sustain *T. brucei* growth *in vitro*

Mice infected with *T. brucei* present an increase in adipocyte lipolysis and a progressive reduction of fat mass (Machado *et al*, unpublished data). Given the proximity of parasites and adipocytes in the AT, we hypothesized that *T. brucei* could induce lipolysis through direct contact with the adipocytes. To investigate the influence of *T. brucei* in adipocyte lipolysis, the 3T3-L1 mouse adipocyte cell line was used as *in vitro* model of white adipocytes. This cell line is frequently used to study adipocyte physiology (e.g., adipogenesis and lipolysis) and metabolic diseases. Moreover, it allows for the elimination of confounding factors that exist in an *in vivo* model and offers a homogenous cell population at the same differentiation stage[93,94]. 3T3-L1 preadipocytes present a fibroblast-like morphology (Figure 6B) and are already committed to the adipocyte lineage[93,94].

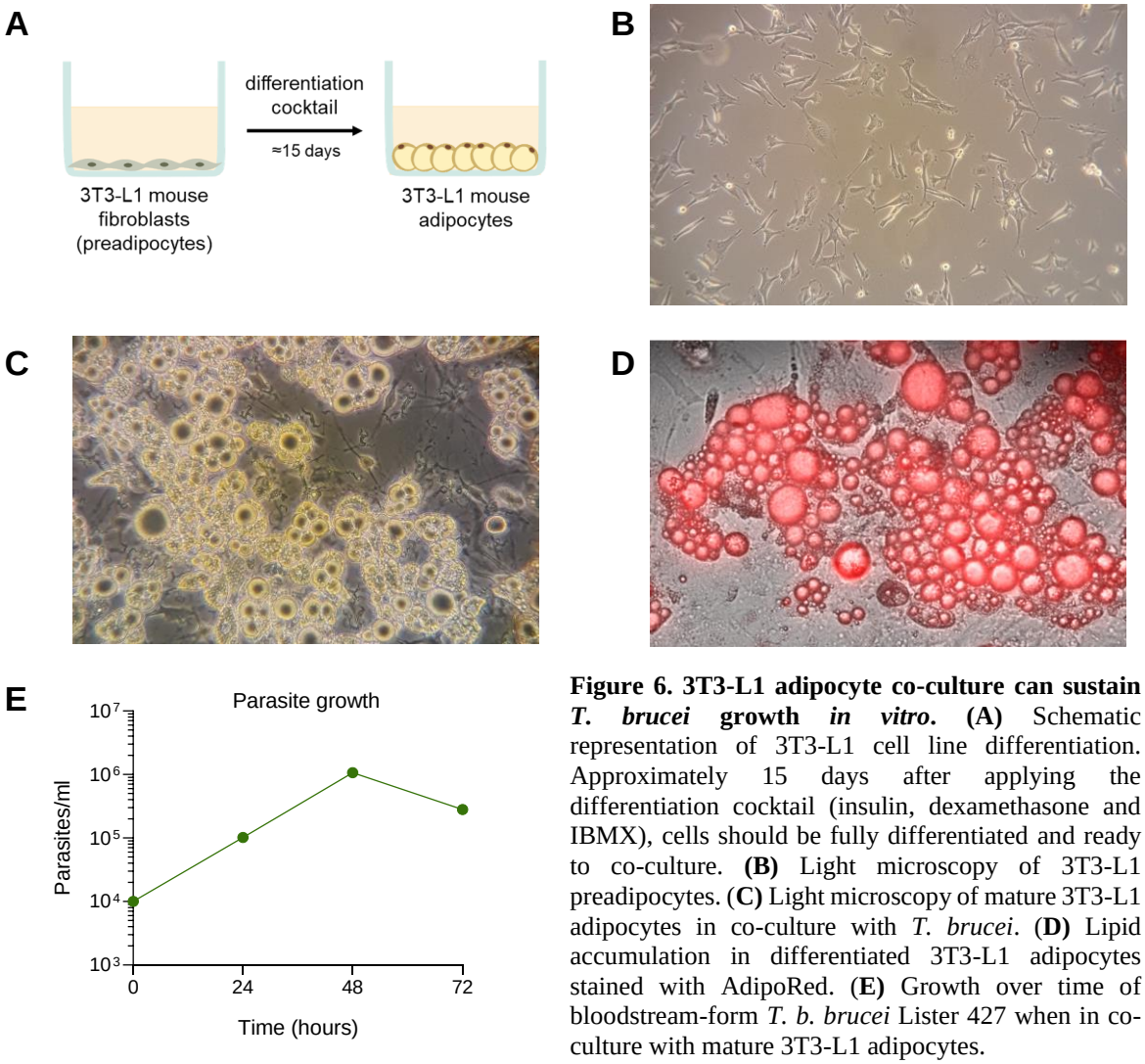


**Figure 6. 3T3-L1 adipocyte co-culture can sustain *T. brucei* growth *in vitro*. (A)** Schematic representation of 3T3-L1 cell line differentiation. Approximately 15 days after applying the differentiation cocktail (insulin, dexamethasone and IBMX), cells should be fully differentiated and ready to co-culture. **(B)** Light microscopy of 3T3-L1 preadipocytes. (**C)** Light microscopy of mature 3T3-L1 adipocytes in co-culture with *T. brucei*. (**D)** Lipid accumulation in differentiated 3T3-L1 adipocytes stained with AdipoRed. (**E)** Growth over time of bloodstream-form *T. b. brucei* Lister 427 when in co-culture with mature 3T3-L1 adipocytes.

For these cells to acquire the characteristics of a mature adipocyte they must undergo terminal differentiation. This process is accomplished by giving confluent preadipocytes a differentiation cocktail of adipogenic agents (Figure 6A): insulin, dexamethasone and IBMX[93,94]. This way adipocytes accumulate TAGs and cytoplasmic lipid droplets are formed, which can be observed by light microscopy (Figure 6C) and fluorescence microscopy (Figure 6D).

*T. b. brucei* strain Lister 427 is a monomorphic strain and was used in all experiments mentioned below unless otherwise mentioned. Lister 427 parasites lost the ability to differentiate into stumpy forms and thus are present exclusively in the slender form. Axenic cultures of *T. brucei* cannot be maintained with standard culture media routinely used for mammalian cell culture (e.g., DMEM). Under these conditions, *T. brucei* requires feeder cells capable of maintaining a low concentration of essential but highly toxic cysteine from cystine reduction[95,96]. To validate the co-culture system, $1x10^4$ *T. brucei* parasites were inoculated in 3T3-L1 adipocytes and live parasites were counted every 24h for 3 days (Figure 6E). No passages were performed during the full length of the experiment. Parasite density increased approximately 10-fold every 24h in the first 48h, which indicates that they can grow and divide in a co-culture system with 3T3-L1 adipocytes for at least two days. After 48h the culture contained dying cells and, as a result, we observed a decrease in parasite density. Given that the Lister 427 strain cannot differentiate into stumpy forms when high parasite densities are reached, we speculate that after 2 days the co-culture medium was either depleted of an essential nutrient or it contained a toxic component that affected parasite growth.

### 3.2. 3T3-L1 adipocytes co-cultured with *T. brucei* show increased lipolysis

To investigate how the presence of *T. brucei* impacted adipocyte lipolysis *in vitro*, we measured the release of lipolytic products by the adipocyte. There are several ways in which we can measure lipolysis. Quantification of NEFAs and glycerol released directly in culture media is the most direct method[97].

After 24h of co-culturing adipocytes and parasites, two further incubations were performed corresponding to two different lipolytic states: basal and stimulated (Figure 7A). For measurement of lipolytic products under the basal condition, DMEM with BSA was added to the cell culture and incubated for 2h. BSA acts as a NEFA acceptor[97]. Without BSA, NEFAs released through lipolysis would be taken up by the adipocyte[97,98]. Unlike NEFAs, adipocytes have limited ability to re-integrate glycerol since glycerol kinase has low activity in WAT[98]. For this reason, variations in glycerol would give a more accurate estimate of the level of lipolysis in adipocytes. However, *T. brucei* also has the glycerol kinase enzyme and can synthesize glycerol. Thus, the total glycerol levels in the medium could originate not only from adipocytes, but also from the parasites.

We co-cultured adipocytes with two different parasite inocula encompassing the multiplicity of infection observed *in vivo* in the gWAT (Mariana de Niz, unpublished data). NEFA and glycerol release

rates were significantly increased when adipocytes were inoculated with $1x10^7$ parasites. Yet, the amount of released glycerol was similar in co-cultures with $1x10^6$ and $1x10^7$ parasites.

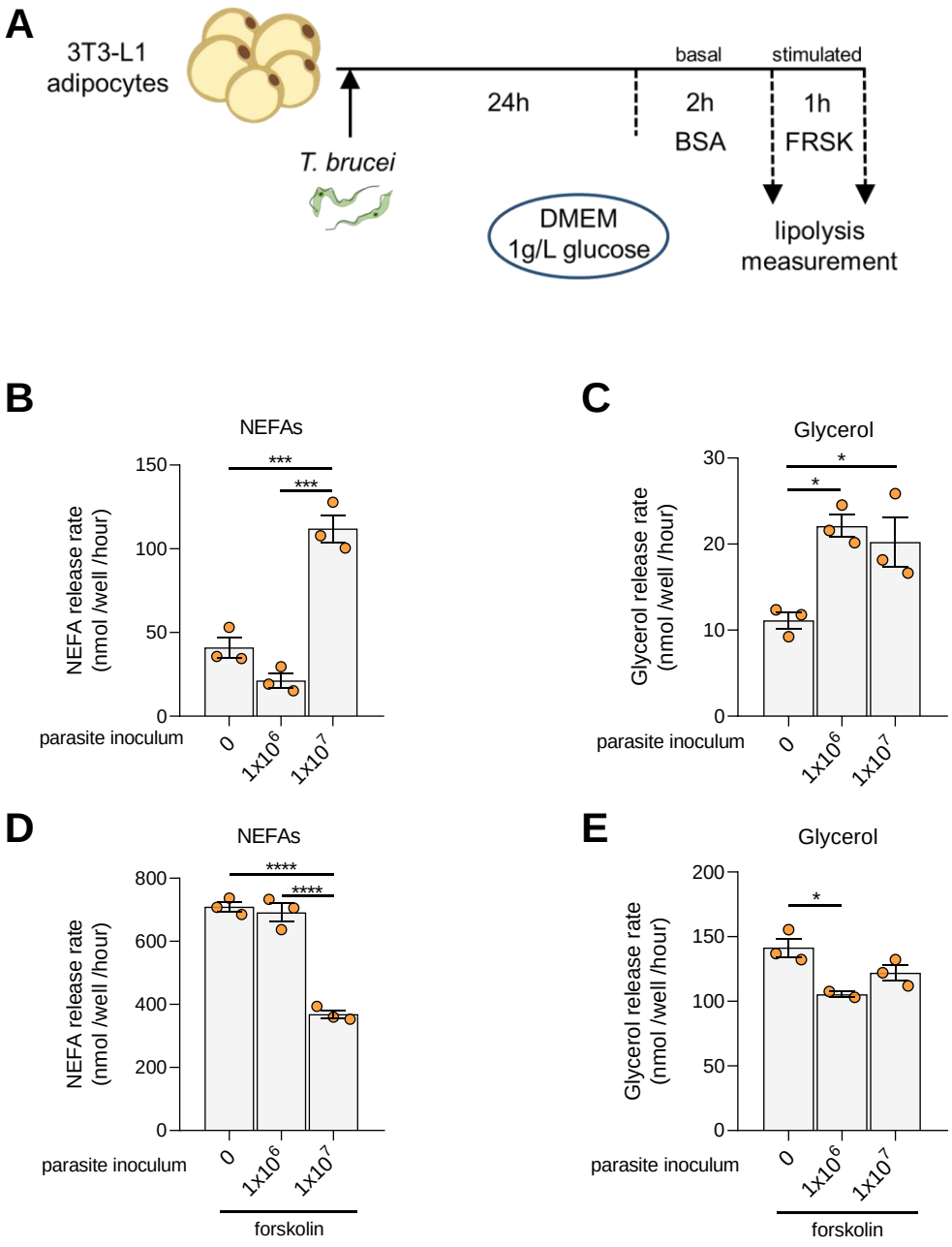


**Figure 7. 3T3-L1 adipocytes co-cultured with *T. brucei* show increased lipolysis. (A)** Schematic representation of the method used for measurement of lipolytic products. Mature 3T3-L1 adipocytes were infected with *T. brucei* and incubated for 24h. After 24h, two additional incubations were performed. The basal condition corresponds to the release of lipolytic products by adipocytes under the sole presence of parasites. The stimulated condition corresponds to release of lipolytic products by adipocytes after stimulation with forskolin (FRSK). **(B)** NEFA release rate (nmol/well/hour) of 3T3-L1 adipocytes after co-culture with *T. brucei* for 24h. (**C)** Glycerol release rate (nmol/well/hour) of 3T3-L1 adipocytes after co-culture with *T. brucei* for 24h. (**D)** NEFA release rate (nmol/well/hour) of 3T3-L1 adipocytes after stimulation with 10 µM forskolin. **(E)** Glycerol release rate (nmol/well/hour) of 3T3-L1 adipocytes after stimulation with 10 µM forskolin. One experiment conducted in biological triplicates. Data are presented as mean ± SEM. One-way ANOVA with Sidak post hoc test was

performed to compare experimental groups. Significance is expressed as ****p < 0.0001, ***p < 0.001, **p < 0.01 or *p < 0.05.

To assess whether adipocytes remained responsive after *T. brucei* co-culture, we measured lipolytic products for 1 hour under forskolin stimulation. Forskolin is a plant bioactive compound found in *Coleus forskohlii* and acts by enhancing adenylate cyclase activity and increasing intracellular cAMP levels in the adipocyte[99], leading to PKA-mediated lipolysis. Overall, 3T3-L1 adipocytes treated with forskolin have considerably higher lipolytic product release rates comparing to the basal condition, which indicates that adipocytes are responsive to stimuli. Forskolin-stimulated adipocytes in co-culture show a decrease in lipolytic product release rates when compared to the non-infected adipocytes (Figure 7D and 7E), suggesting that adipocytes are less responsive to increase in cAMP levels after being in co-culture with *T. brucei*.

Collectively, these data show that *T. brucei* is able to induce adipocyte lipolysis.

### 3.3. Expression of lipolytic enzymes is not significantly altered during infection

For release of NEFAs and glycerol, TAGs packed in the lipid droplet need to be hydrolyzed into its components. This process is called 'neutral lipolysis' and is mediated by three lipases. To understand the mechanism underlying the release of lipolytic products during infection, we analyzed transcript levels, protein content and activation levels of the main neutral lipases.

Transcript levels were measured by RT-qPCR. First, we selected four housekeeping genes to test if they would be suitable normalizers: *Gapdh* (glyceraldehyde 3-phosphate dehydrogenase), *Hprt* (hypoxanthine-guanine phosphoribosyl transferase), *β-actin* and *18S rRNA* (Figure 8). We chose these genes because they are some of the most commonly used normalizers in RT-qPCR analysis.

Cycle threshold (Ct) values of most housekeeping genes varied significantly in tested conditions, especially between the uninfected and infected groups. This is a problem because internal reference genes need to have stable transcript levels and cannot be affected by experimental conditions[100,101]. However, this also suggests that infection by *T. brucei* induces changes in overall adipocyte metabolism.

Altogether, in co-culture conditions, housekeeping genes tend to have higher Ct values, which translates into lower amounts of target cDNA (Figures 8B, 8C and 8D). The most dramatic variability between tested conditions is observed with *18S rRNA*, which presented a difference of 6 Ct values (Figure 8D). Thus, for the remaining analysis, *Gapdh* was used as the normalizer gene since there is a lower standard error of the mean in each experimental condition and the difference between means is less than one Ct (Figure 8A).

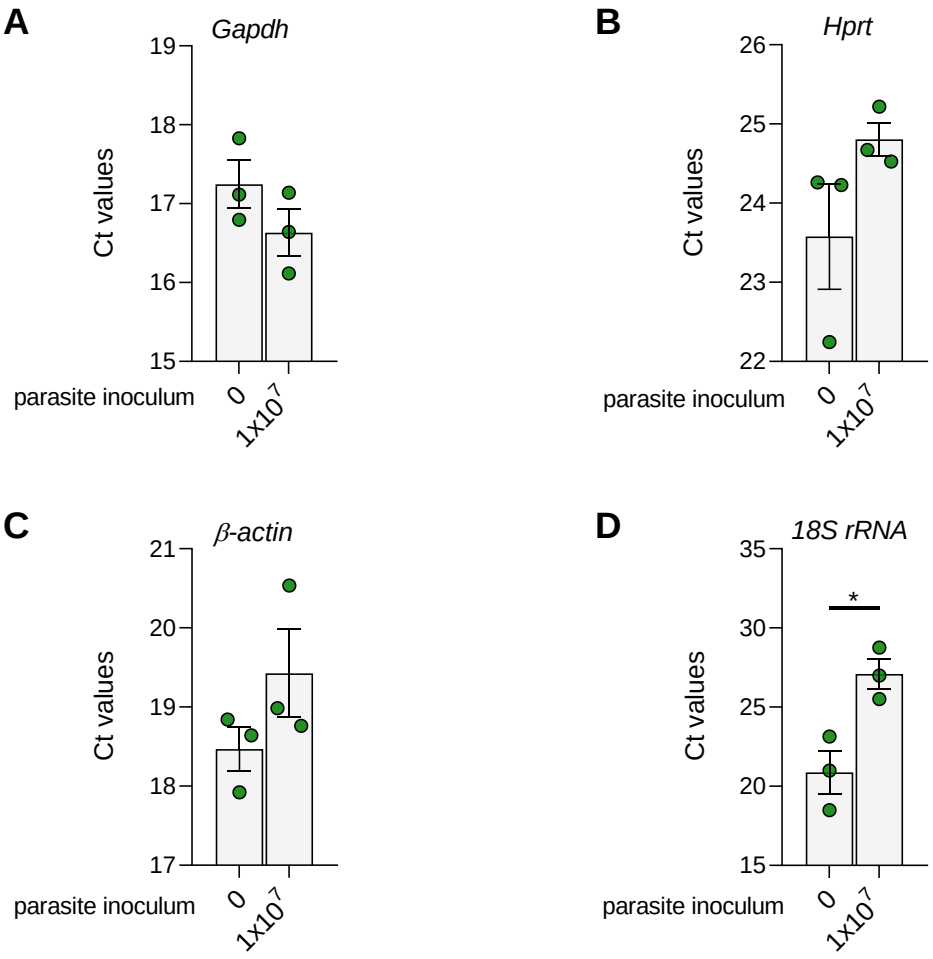


**Figure 8. Transcript levels of housekeeping genes vary among experimental conditions. (A-D)** RT-qPCR Ct values of **(A)** *Gapdh*, **(B)** *Hprt*, **(C)** *β-actin*, **(D)** *18S rRNA* in non-infected and infected 3T3-L1 adipocytes after 24h. Representative of two independent experiment, conducted in biological triplicates. Data are presented as mean ± SEM. Two-way t-Student test was performed to compare experimental groups. Significance is expressed as *p < 0.05.

The mobilization of TAGs from the lipid droplet is made sequentially by three lipases (Figure 4): ATGL, HSL and MGL. ATGL and HSL are the rate-limiting enzymes in the lipolytic pathway, responsible for more than 95% of the hydrolase activity in mouse WAT[102]. After 24h, co-culture with *T. brucei* did not significantly change the transcript levels of *Pnpla2* (ATGL; Figure 9A), *Lipe* (HSL; Figure 9B) or *Mgll* (MGL; Figure 9C). In a similar way, expression of the lipogenic gene that encodes fatty acid synthase (FAS; *Fasn* gene) was not altered by the presence of the parasites (Figure 9D).

Additionally, we also tested the hypothesis of lipolysis occurring by an alternative pathway. The *Lipa* gene encodes LAL, the enzyme that mediates lipophagy and can also lead to NEFA release through 'acid lipolysis'. However, our RT-qPCR analysis showed that mRNA levels of *Lipa* are similar in the presence and absence of parasites, suggesting that transcription regulation of LAL was not responsible for the increase in release of lipolytic products (Figure 9E).

Taken together, RT-qPCR data indicate that the transcript levels of enzymes associated with adipocyte lipolysis and lipogenesis are not altered by the presence of *T. brucei*.

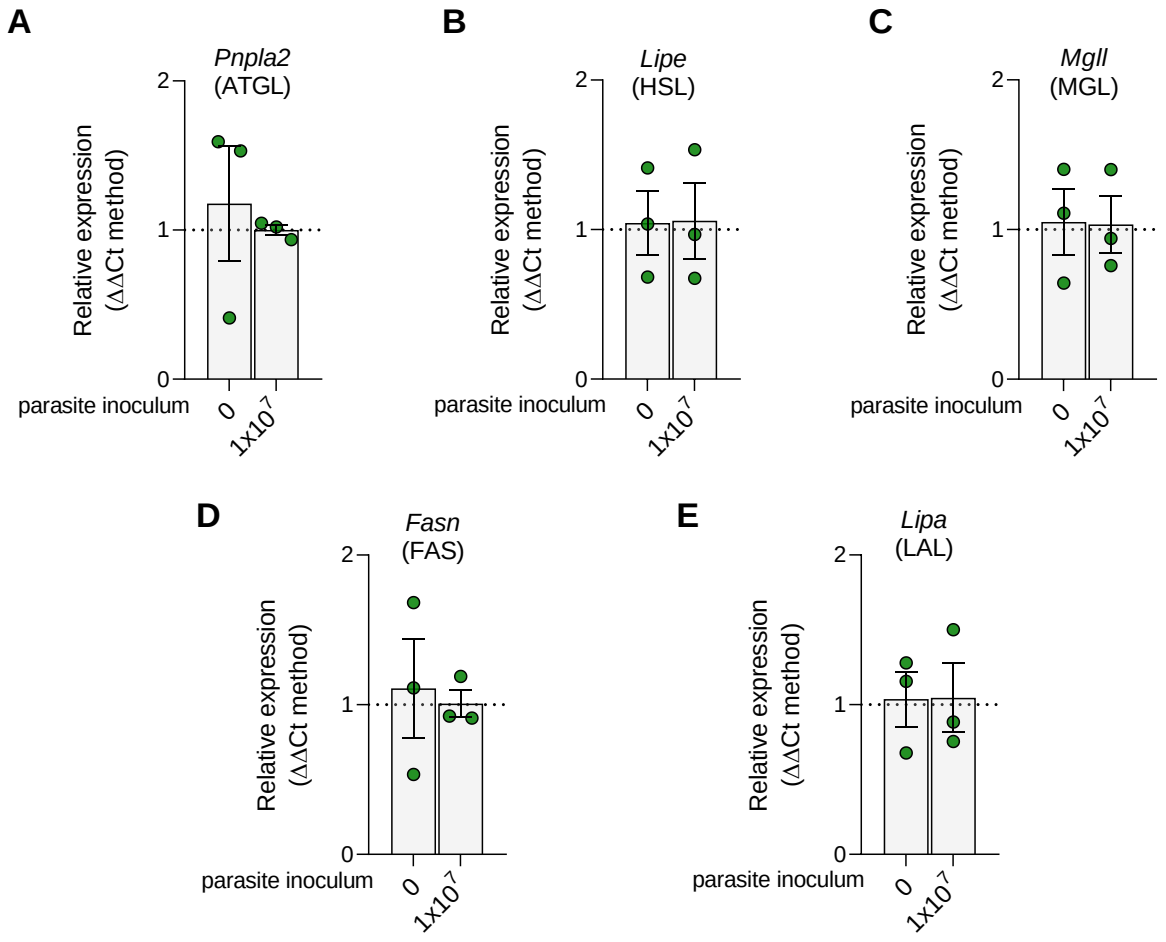


**Figure 9. Gene expression levels of adipocyte metabolism enzymes are not altered during infection. (A-E)** Relative expression of **(A)** *Pnpla2* (ATGL), **(B)** *Lipe* (HSL), **(C)** *Mgll* (MGL), **(D)** *Fasn* (FAS) and **(E)** *Lipa* (LAL) in non-infected and infected 3T3-L1 adipocytes after 24h. Representative of two independent experiments, conducted in biological triplicates. Data are presented as mean ± SEM. Two-way t-Student test was performed to compare experimental groups.

Next, we checked the protein and activation levels of the main neutral lipases. We started by examining total ATGL, the first and rate-limiting enzyme in the lipolytic pathway. For that, we used western blotting analysis with an antibody against ATGL[103]. We found that the levels of ATGL protein remained unchanged in the presence or absence of *T. brucei* parasites in co-culture (Figures 10A and 10B).

Afterwards, we assessed the activation levels of HSL, the second enzyme in the lipolytic pathway which is subjected to post-translational modifications that affect lipolysis. HSL can be enzymatically phosphorylated in five different serine residues causing either activation or inhibition. In mice, activation of HSL by PKA is mediated by phosphorylation on three distinct serine residues: Ser[563], Ser[659]

and Ser[660]. Each site has a different regulatory role: while phosphorylation at Ser[659] and Ser[660] is thought to be activation of intrinsic enzymatic activity[59,104], the functional significance of phosphorylation at Ser[563] is not completely elucidated, but it is thought to mediate translocation of HSL to the lipid droplet[105]. Activation of HSL can also be promoted by phosphorylation of Ser[660] by ERK[59]. Contrarily, phosphorylation of mice HSL on Ser[565] by AMP-activated protein kinase (AMPK) has an inhibitory effect, blocking translocation of HSL to the lipid droplet[59]. Here, we detected levels of HSL only when phosphorylated at Ser[563] by PKA (pHSL) by western blot using the Phospho-HSL (Ser[563]) specific antibody[103]. We observed that HSL activation on Ser[563] remained constant with both parasite inocula and it was not significantly different from adipocytes cultured in the absence of *T. brucei* (Figures 10C and 10D).

Altogether, our analysis reveals that there is no altered protein expression or activation of lipases during *T. brucei* infection.

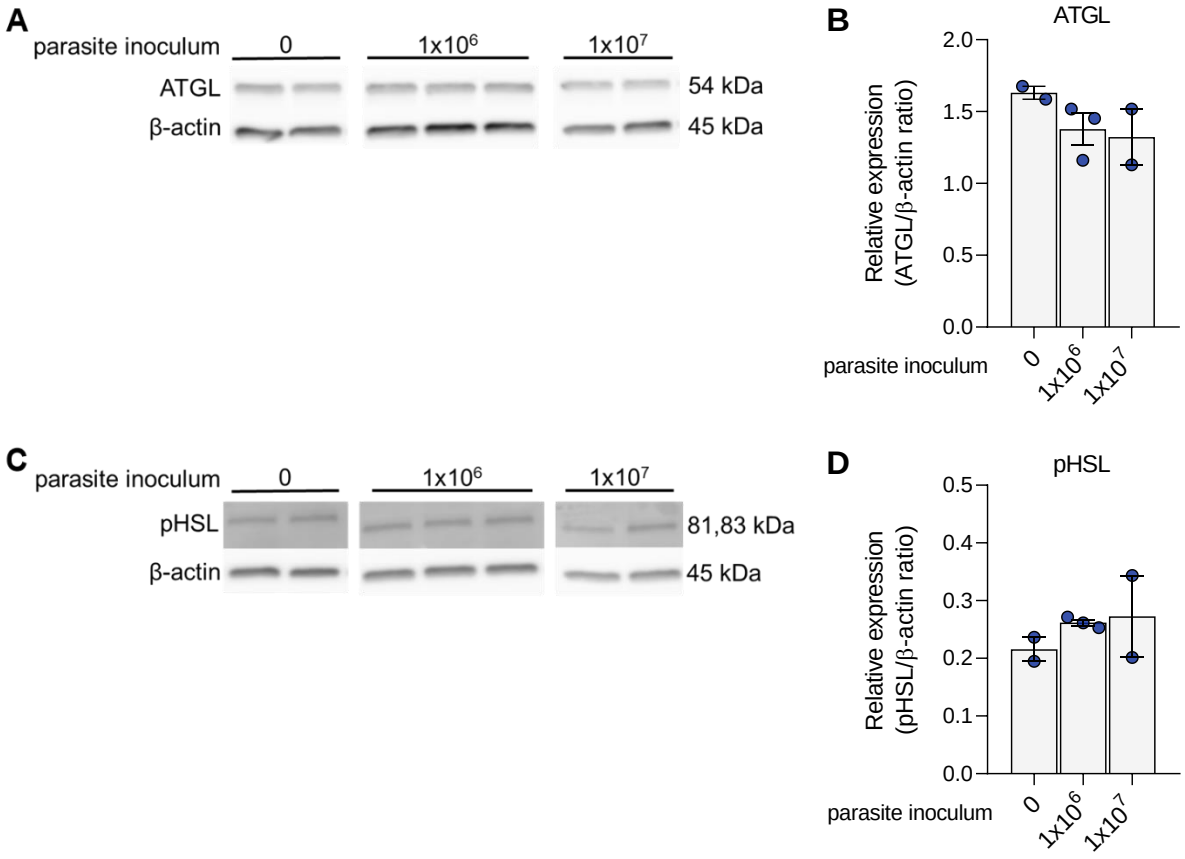


**Figure 10. ATGL protein content and HSL activation are not altered during infection. (A)** Western blot of ATGL in non-infected and infected 3T3-L1 adipocytes after 24h. β-actin was used as loading control. (**B)** Quantification of ATGL protein levels in non-infected and infected 3T3-L1 adipocytes after 24h. **(C)** Western blot of pHSL Ser[563] in non-infected and infected 3T3-L1 adipocytes after 24h. β-actin was used as loading control. (**D)** Quantification of pHSL Ser[563] protein levels in non-infected and infected 3T3-L1 adipocytes after 24h. ATGL data are representative of two independent experiments. Data are presented as mean ± SEM. One-way ANOVA with Sidak post hoc test was performed to compare experimental groups.

### 3.4. Lipolysis increase is not reproduced in the adipose tissue explant co-culture

To verify if the increased release of lipolytic products phenotype was reproducible, we tested a different adipose model namely AT explant co-cultures.

gWAT was isolated from non-infected male C57BL/6 mice and infected *in vitro* with two different *T. brucei* inocula. gWAT of male mice is one of the largest depots in rodents and is usually used to represent visceral WAT[106]. Tissue explants represent a more physiological model and a closer reproduction of the *in vivo* condition, maintaining the different cell populations present in the AT, the extracellular matrix and paracrine interactions that may influence adipocyte metabolism[107]. Yet, explant cultures have some disadvantages: diffusion of metabolic products from the center of the tissue and dissemination of parasites to the center of the tissue might be impaired, there is greater variability in results and different depots differ in metabolic patterns[93,108].

After a 24h incubation, lipolytic products were quantified according to the same system established for the 3T3-L1 cell culture. NEFA release rate did not show significant differences between the non-infected condition and both parasite inocula used (Figure 11A). On the other hand, glycerol release rate showed a significant 1.5-fold increase when explants were infected with $1x10^7$ parasites (Figure 11B), which may be of parasite origin and not a product of adipocyte lipolysis.

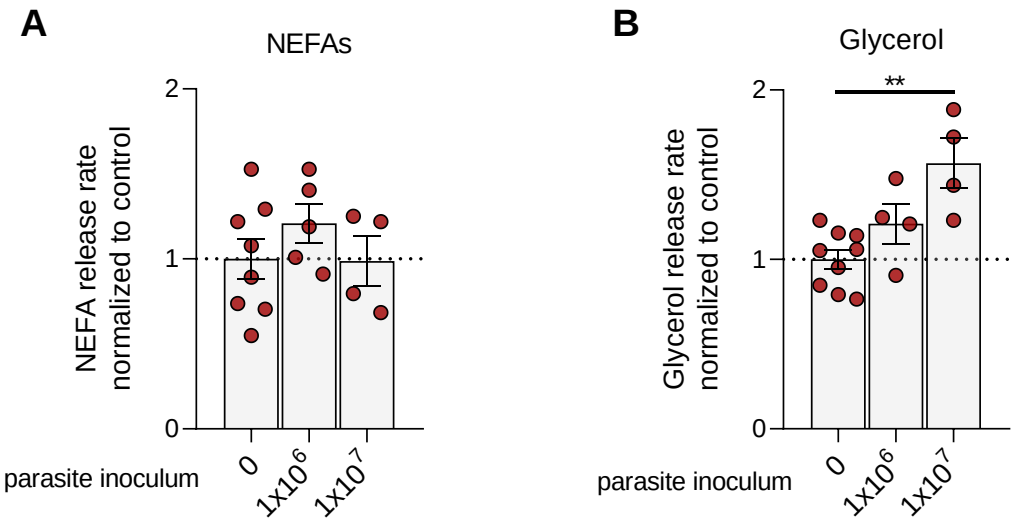


**Figure 11. Lipolysis increase is not reproduced in the adipose tissue explant co-culture. (A)** NEFA release rate of *T. brucei* infected and non-infected gWAT explants from C57BL/6 mice after 24h incubation. Data shown are from two independent experiments, each experimental group is normalized to the respective non-infected control group. (**B)** Glycerol release rate of *T. brucei* infected and non-infected gWAT explants from C57BL/6 mice after 24h incubation. Data shown are from two independent experiments, each experimental group is

normalized to the respective non-infected control group. Representative of two independent experiments. Data are presented as mean ± SEM. One-way ANOVA with Sidak post hoc test was performed to compare experimental groups. Significance is expressed as **$p < 0.01$.

### 3.5. Live parasites are not essential for the increase in lipolytic product release

We next questioned whether the increased lipolytic rate observed for 3T3-L1 adipocytes co-cultured with *T. brucei* required the presence of live parasites. Hypothesizing that engagement of PRRs on the surface of adipocytes with *T. brucei* was the lipolytic trigger, supplying the respective PAMPs should lead to an increase in the release of lipolytic products. Indeed, 3T3-L1 adipocytes express many PRRs and are responsive to TLR-2/1, TLR-3, TLR-4, TLR-2/6 and TLR-9 agonists[65,109,110]. Accordingly, if this hypothesis is correct stimulation of adipocytes with a crude lysate of *T. brucei* should lead to activation of lipolysis.

*T. brucei* lysates were obtained by subjecting parasites to several freeze-thaw cycles, thus the lysate is a complex mixture containing DNA, RNA, proteins and lipids. The parasite lysate protein content is visible in the SDS-PAGE gel represented in Figure 12A, showing a wide range of protein sizes. As expected, the most prominent band has a molecular weight close to 50 kDa which coincides with the expected molecular weight of variant surface glycoprotein (VSG). The lysates tested differed in the initial number of parasites lysed.

After 6h, there is a significant increase in NEFA release (1.6-fold) and glycerol release (1.4-fold) when adipocytes are incubated with lysates prepared from $5x10^6$ parasites (Figures 12B and 12C). Incubation of *T. brucei* lysates with adipocytes did not increase lipolytic product release rates significantly after 24h (Figures 12B and 12C), although a positive trend (2-fold increase compared to non-infected adipocytes) was observed for NEFA release in adipocytes stimulated with lysates prepared from $5x10^6$ parasites (Figure 12B). The increase in NEFA release with $5x10^6$ lysed parasites seems to be maintained over time with a similar fold increase (Figure 12B).

Regarding the live parasite positive control, we observed a 2-fold increase in NEFA release in adipocytes cultured with $1x10^7$ live parasites at 6h. After 24h, the positive control corroborated results presented in Figure 7, with NEFA release being significantly increased again (7-fold) (Figure 12B). Curiously, glycerol release over time in co-cultures with live parasites displays an inverted pattern when compared to NEFA. Release rates for glycerol have a peak at 6h (3-fold increase compared to non-infected adipocytes) while at 24h they presented only a 1.5-fold increase over the non-infected adipocytes (Figure 12C). Overall, results indicate that parasite lysates are not as efficient as live parasites at inducing adipocyte lipolysis.

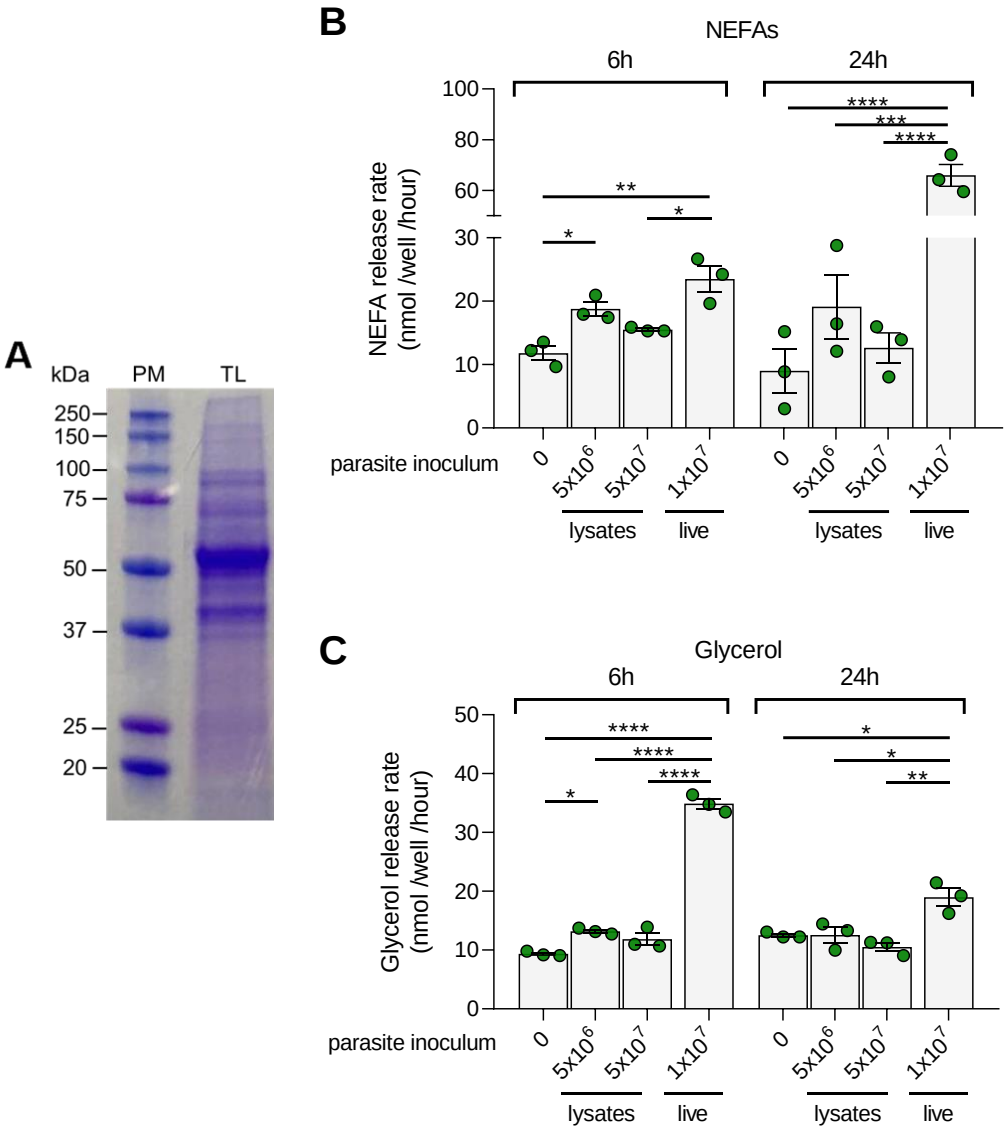


**Figure 12. Live parasites are not essential for the increase in lipolytic product release. (A)** Total parasite lysate proteins visualized by SDS-PAGE with Coomassie blue staining. PM, protein marker; TL, total lysate. **(B)** NEFA release rate (nmol/well/hour) of 3T3-L1 adipocytes after co-culture with *T. brucei* lysates for 6h and 24h. Live parasite condition was used as positive control. (**C)** Glycerol release rate (nmol/well/hour) of 3T3-L1 adipocytes after co-culture with *T. brucei* lysates for 6h and 24h. Live parasite condition was used as positive control. Representative of two independent experiments, conducted in biological triplicates. Data are presented as mean ± SEM. One-way ANOVA with Sidak post hoc test was performed to compare experimental groups. Significance is expressed as ****p < 0.0001, ***p < 0.001, **p < 0.01 or *p < 0.05.

### 3.6. Physical contact between adipocytes and *T. brucei* enhances adipocyte lipolysis

We have shown that live parasites are more efficient than crude lysates at inducing adipocyte lipolysis. Next, we investigated if this induction of lipolysis requires direct physical contact or whether it is mediated by a soluble factor. To achieve this, we implemented a transwell system, where a monolayer of 3T3-L1 adipocytes was cultured on the bottom

compartment and, according to the condition tested, parasites would be added to the transwell insert (IN) or to the adipocyte monolayer (OUT) (Figure 13A). The transwell membrane (0.4 µm pore size) allows for the passage of soluble molecules but is not permeable to trypanosomes since slender bloodstream forms have approximately 3 µm width[111].

After 24h of incubation, adipocytes co-cultured with *T. brucei* inside and outside the transwell with the same initial inoculum showed a different pattern of lipolytic product release (Figure 13B and 13C). NEFA release rate was significantly increased between infected adipocytes in direct contact with trypanosomes and the non-infected control (15-fold) (Figure 13B). We also observed a trend for increased NEFA release in adipocytes co-cultured with trypanosomes inside the transwell (5-fold) (Figure 13B).

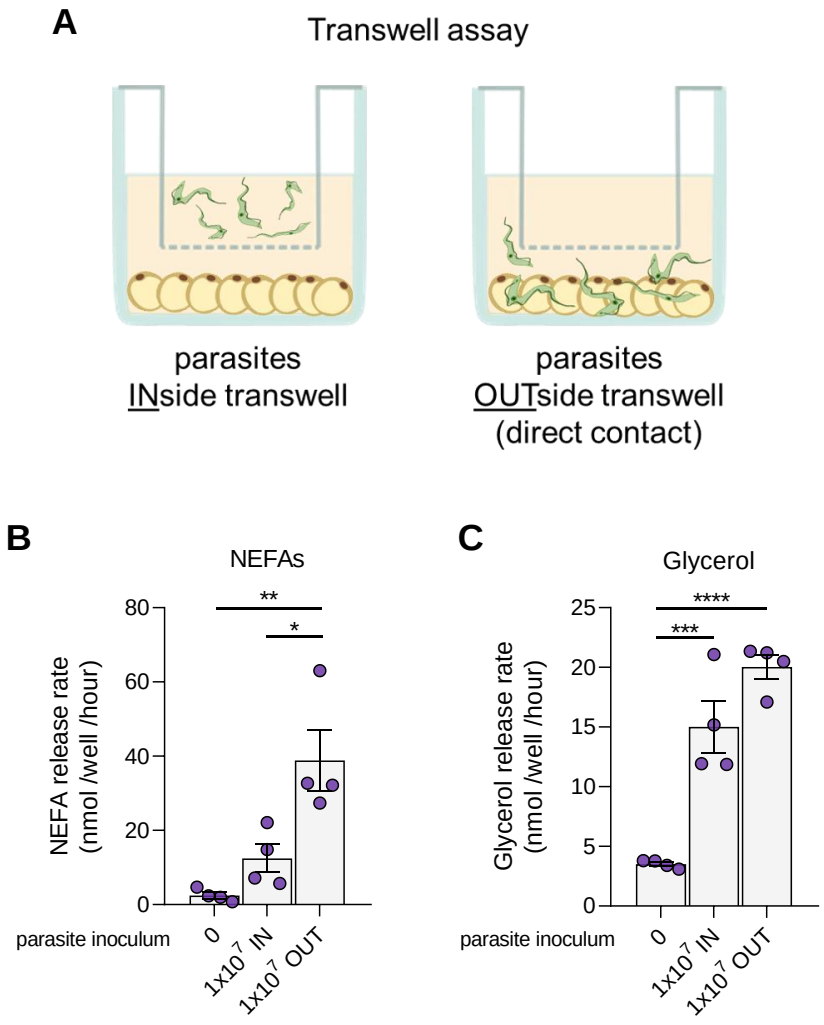


**Figure 13. Physical contact between adipocytes and T. brucei enhances adipocyte lipolysis. (A)** Schematic representation of the transwell assay implemented to study the influence of direct contact between parasites and adipocytes on lipolysis. (**B)** NEFA release rate (nmol/well/hour) in non-infected and infected 3T3-L1 adipocytes after 24h. Parasites were inoculated inside (IN) or outside (OUT) the transwell insert. (**C)** Glycerol release rate

(nmol/well/hour) in non-infected and infected 3T3-L1 adipocytes after 24h. Parasites were inoculated inside (IN) or outside (OUT) the transwell insert. One experiment conducted in biological triplicates. Data are presented as mean ± SEM. One-way ANOVA with Sidak post hoc test was performed to compare experimental groups. Significance is expressed as ****p < 0.0001, ***p < 0.001, **p < 0.01 or *p < 0.05.

Glycerol release rates between the infected conditions were not significantly different from each other but both were higher than the non-infected cultures: 4-fold increase when parasites were inoculated inside the transwell and 5.6-fold increase when parasites were cultured outside the transwell (Figure 13C). Interestingly, adipocytes co-cultured with *T. brucei* inside the transwell insert presented a high rate of glycerol release, as in this case parasites were no longer present during the measurement stage. Thus, increased glycerol levels detected in these co-cultures are likely of bona fide adipocyte lipolysis origin.

Overall, results indicate that when parasites directly contact adipocytes there is an enhancement of lipolytic product release by adipocytes. However, there is a trend for NEFA release to be increased when parasites are not contacting adipocytes which can suggest that, besides direct contact, a soluble factor may also have a contribution to lipolysis stimulation.

### 3.7. Inhibition of ATGL during infection reduces adipocyte lipolysis

Next, we examined whether the lipolysis increase observed in 3T3-L1 co-cultures was dependent on ATGL activity, as observed during an *in vivo T. brucei* infection (Machado *et al*, unpublished). Here, atglistatin was used as a specific inhibitor of mice ATGL having no activity against HSL or MGL[112]. Release rates of lipolytic products in the presence and absence of the inhibitor were then measured and compared to determine the involvement of ATGL activity during infection. Non-infected conditions in groups treated and non-treated with atglistatin showed a significant decrease in lipolytic product release, which indicates that inhibition was successful (Figures 14).

While co-culturing adipocytes and *T. brucei* led to an increase in NEFA release (1.8-fold), addition of atglistatin reduced NEFA release rates to levels comparable to those exhibited by non-infected adipocytes with inhibited ATGL (Figure 14A).

Contrarily, glycerol release by infected adipocytes in the presence of the ATGL inhibitor is still significantly increased when compared to non-infected adipocytes (Figure 14B). Nonetheless, infected adipocytes with inhibited ATGL presented significantly reduced glycerol release rates when compared to adipocytes with non-inhibited ATGL (Figures 14B). After

inhibition of the rate-limiting enzyme in lipolysis there is still a significant amount of glycerol being detected, this is most likely from parasite origin. Nevertheless, although parasites may be contributing to measured glycerol, this does not correspond to the totality of glycerol quantified in the absence of atglistatin. Taken together, this indicates that glycerol is also coming from adipocytes.

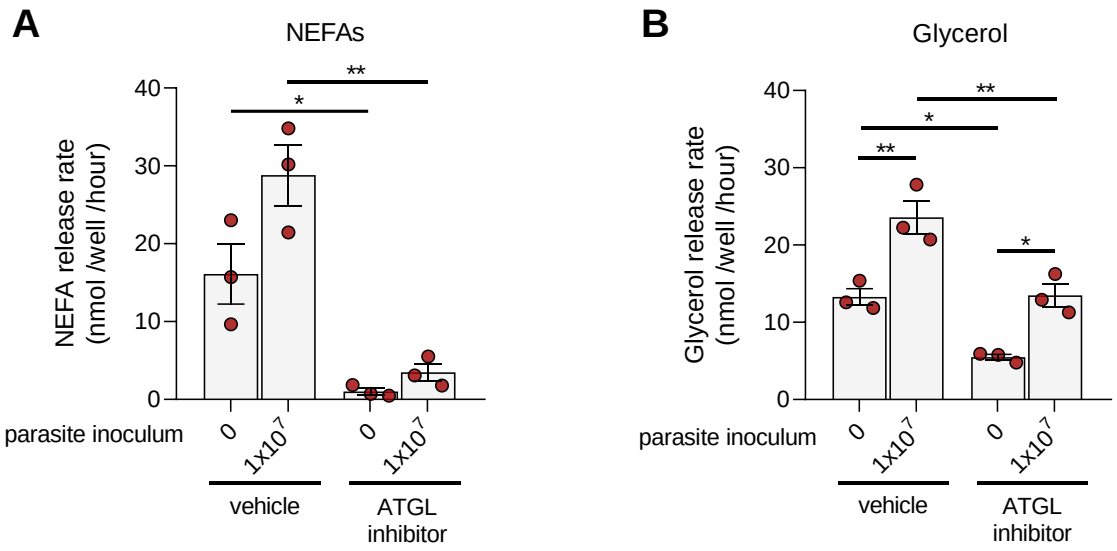


**Figure 14. Inhibition of ATGL during infection reduces adipocyte lipolysis. (A)** NEFA release rate (nmol/well/hour) in non-infected and infected 3T3-L1 adipocytes treated with atglistatin (ATGL inhibitor) or DMSO (vehicle) after 24h. (**B)** Glycerol release rate (nmol/well/hour) in infected and non-infected 3T3-L1 adipocytes treated with atglistatin (ATGL inhibitor) or DMSO (vehicle) after 24h. One experiment conducted in biological triplicates. Data are presented as mean ± SEM. One-way ANOVA with Sidak post hoc test was performed to compare experimental groups. Significance is expressed as **$p < 0.01$ or *$p < 0.05$.

# 4. Discussion and future perspectives

AT can harbor several pathogens with different consequences for host and invader microorganism. Some of these pathogens can use AT as a reservoir, this is the case of *T. brucei*. Prior work identified mice AT as a major reservoir of parasites. Moreover, establishment of *T. brucei* was accompanied by alterations in the tissue which suggested the mobilization of lipids stored in the adipocyte. Taking in consideration the evidence mentioned, we questioned what type of relation does *T. brucei* establish with host adipocytes and what effect it has in host metabolism. Here, we investigated how the interaction between *T. brucei* and adipocytes influences adipocyte lipolysis using an *in vitro* model.

We found that the presence of parasites in the vicinity of adipocytes was associated with a substantial increase in the release of lipolytic products, which correlates to an increase in lipolysis (Figure 7). Furthermore, there were no changes in the phenotype between the monomorphic bloodstream strain Lister 427 and the pleomorphic bloodstream strain AnTat 90:13 (Supplementary figure 1), suggesting that slender forms are sufficient to induce lipolysis in adipocytes. Although both NEFAs and glycerol release rates were increased in infected adipocytes, glycerol measurements are not the most accurate to use as proxy for lipolysis since parasites are intertwined in the adipocyte monolayer during measurement incubations and they may secrete glycerol to the medium. Given that there is no evidence that *T. brucei* secretes significant amounts of NEFAs, we conclude that NEFAs measurements are the most reliable indicator of adipocyte lipolysis. Additionally, inhibiting ATGL in infected adipocytes abates the release of NEFAs, further supporting their adipocyte origin (Figure 14).

## 4.1. Lipase regulation

Contrary to what we expected, transcript levels of the lipases in the lipolytic cascade (*Pnpla2*, *Lipe* and *Mgll*) were not altered in adipocytes co-cultured with *T. brucei* (Figure 9). In a similar way, ATGL levels detected by western blot did not show any changes in infected adipocytes (Figure 10). Although we observed an increase in the release of lipolytic products, this did not reflect an increase in lipase mRNA and protein levels. Lipases in WAT can be regulated at several stages. Besides gene expression and translation, other factors like subcellular localization, post-translational modifications and interaction with regulatory proteins might affect their activity[97]. Studies that study lipase activity during endurance exercise *in vivo*[113,114] or in response to lipolysis-inducing stimuli *in vitro*[115] have described cases where TAGs are being mobilized but there is no increase in ATGL or HSL protein or mRNA levels. For example, Kralisch *et al.* has shown that TNF-α, a powerful activator of lipolysis, downregulates mRNA levels of ATGL and HSL in a dose and time-dependent manner in 3T3-L1

adipocytes[115]. In the same study, forskolin, a lipolysis-inducing molecule which we use as positive control for adipocyte responsiveness, also downregulates ATGL mRNA expression[115]. This suggests that lipolytic enzymes are mainly regulated at a post-transcriptional level, which makes lipase transcript measurements an inadequate marker for lipase activity in many biological conditions[97,116].

Other methods that allow for a more accurate study of lipase activity include knockout or knockdown of lipase genes and lipase-specific inhibitor molecules. Here, atglistatin was used as an inhibitor of mice ATGL, the rate-limiting enzyme in the lipolytic pathway. Atglistatin does not interfere in the interaction between ATGL and its activator (i.e., CGI-58) nor does it displace ATGL from the lipid droplet[112]. Adipocytes with inhibited ATGL co-cultured with *T. brucei* showed a dramatic decrease in NEFAs release in comparison to infected adipocytes with non-inhibited ATGL (Figure 14). These results allowed to conclude that *T. brucei* induced lipolysis is ATGL-dependent.

Similarly, other specific inhibitors directed at different steps of the lipolytic pathway could be used to characterize the molecular mechanism that leads to increased lipolysis during infection. HSL-specific inhibitor BAY or NNC0076-0079 and MGL-specific inhibitor JZL184 could be used to determine the contribution of each lipase to the lipolytic pathway in the context of infection. Nonetheless, inhibition of MGL would only determine MGL-independent MAG hydrolase activity since HSL can partially compensate MGL activity. Additionally, inhibition of PKA using a specific inhibitor, like protein kinase inhibitor peptide (PKI) could also be used to investigate if phosphorylation events are PKA-dependent. The current models for regulation of the lipolytic pathway are complex and include several players. Activation of lipolysis through non-canonical pathways has also been described, namely through TLRs and NOD receptors, resulting in activation of different signaling pathways (e.g., ERK pathway)[67,68]. So, analysis of other kinases should also be considered.

To further understand the role of ATGL during adipocyte infection, analysis of the proteins involved in activation (CGI-58) and repression (G0S2) of this lipase should be considered. Interaction between CGI-58 and ATGL is dependent on PLIN1 phosphorylation, so availability of this activator is not only dependent on its expression.

Another important aspect of lipolysis is the spatial regulation of events which involves protein trafficking. Lipolysis occurs at the lipid droplet surface which is covered in PLIN1. PLIN1 coordinates the mobilization and activation of lipases and their access to TAGs. For degradation of TAGs to take place, the lipases must translocate from the cytosol to the lipid droplet, so their action is not only determined by their enzymatic activity but also by their subcellular localization[117]. Accordingly, immunofluorescence analysis should be used to study co-localization of key lipolytic proteins during *T. brucei* infection.

The phosphorylation state of PLIN1 is also a key regulation step in the lipolytic pathway since it influences direct or indirectly ATGL and HSL activity. Besides controlling the access of ATGL to its activator CGI-58, PLIN1 is involved in lipid droplet remodeling for lipase binding and its interaction with HSL is essential for docking of the lipase on the lipid droplet[118]. Given that PLIN1 is an important

player in the lipolytic pathway, further work should contemplate analysis of expression, phosphorylation state and localization of this protein during infection.

As mentioned previously, regulation of HSL is dependent on phosphorylation in specific serine residues and on interaction with PLIN1 on the surface of the lipid droplet. Only phosphorylation at $Ser^{563}$ was analyzed by western blot. HSL activation mediated by this specific residue in infected adipocytes was not different from non-infected adipocytes (Figure 10). Since phosphorylation at $Ser^{563}$ is thought to be involved in translocation of HSL from the cytosol to the lipid droplet, analyzing subcellular localization through immunofluorescence may give additional insight on spatial regulation of HSL during *T. brucei* infection.

Other aspects to consider are the kinetics and transient nature of some post-translation modifications like phosphorylation. When under stimulation with forskolin, phosphorylation at $Ser^{563}$ in 3T3-L1 adipocytes is detected 1 minute after stimulation and it increases over a 30-minute period[119]. On the other hand, phosphorylation at $Ser^{660}$ was detected only 10 seconds after stimulation, proving how quick the kinetics of HSL phosphorylation can be[119]. Since we analyzed phosphorylation levels after 24h, it is feasible that infected adipocyte had already experienced a transient increase in HSL phosphorylation. In the future, shorter incubation times should be employed to study HSL activation in our co-culture model. Lastly, in order to have a more comprehensive understanding of HSL activation, other phosphorylation sites (i.e., $Ser^{660}$ and $Ser^{659}$) should be considered for future analysis by western blot or immunofluorescence.

## 4.2. Balance between anabolism and catabolism

During *T. cruzi* infection in mice, it has also been reported a reduction in AT mass and adipocyte size[86]. González *et al.* suggested that this decrease could be due not to lipolysis increase since expression levels of ATGL and HSL were markedly reduced, but to an imbalance between the rate of lipolysis and lipogenesis[86]. In this situation, we would see a decrease in adipocyte size due to an inability to store TAGs and not to an increase in TAG breakdown.

Lipogenesis includes the process of NEFA esterification into TAGs but also the synthesis and activation of NEFAs[120]. NEFAs used to produce TAGs can be acquired by adipocyte uptake from circulation (NEFAs originated from lipoproteins and recycling of stored NEFAs) or *de novo* synthesis in the adipocyte[121]. Here, we measured gene expression of the central rate-limiting enzyme in *de novo* lipogenesis, FAS (which converts malonyl-CoA into palmitate, the first fatty acid produced)[121]. In our model, *Fasn* transcript levels were not altered in adipocytes co-cultured with *T. brucei* (Figure 9), suggesting that the adipocyte anabolic pathways were not affected by infection. However, given that TAG production can be mediated by different pathways, expression of other lipogenic genes should also be investigated to confirm that lipogenesis in not altered.

This process (i.e., *de novo* lipogenesis) is highly dependent on the availability of glucose. Circulating dietary glucose enters the adipocyte through glucose transporter 4 (GLUT4) and is metabolized during *de novo* lipogenesis for NEFA synthesis[122]. Since glucose levels stimulate the lipogenic pathway, genes involved in the uptake and metabolism of glucose (e.g., glycolysis and tricarboxylic acid cycle) in the adipocyte should also be analyzed.

In addition to NEFAs synthesized by *de novo* lipogenesis, dietary and liver NEFAs are transported to AT as TAGs in spherical aggregates called lipoproteins. Upon arriving at the AT vasculature, luminal lipoprotein lipase (LPL), attached to the endothelium of capillaries, hydrolyzes TAGs to NEFAs for uptake and re-esterification by adipocytes[123]. LPL is produced by adipocytes and secreted to surrounding interstitial spaces. It has an essential role in facilitation of NEFA entry in the adipocyte and TAG clearance from blood[123]. In mice, knockout of LPL results in severe hypertriglyceridemia (high plasma TAG levels)[124]. Increased serum TAGs and hypertriglyceridemia was also a characteristic of *T. brucei* infection in vervet monkeys[125] and HAT patients[35,126]. Besides hypertriglyceridemia, *T. brucei* infected rabbits also showed deficient LPL activity[127]. Consequently, analysis of expression and activity of LPL should also be included in future work.

### 4.3. Lipolytic trigger

Besides examining the mechanistic possibilities that underlie the increase in lipolysis observed when co-culturing adipocytes and *T. brucei*, we also aimed at understanding what type of stimuli triggers adipocyte lipolysis in the presence of *T. brucei*. We showed that direct contact between live parasites and adipocytes significantly enhances the release of lipolytic products. However, when parasites were cultured inside the transwell insert that only allowed for the traffic of soluble molecules, with no contact with adipocytes, there was also a trend for increased lipolysis (Figure 13). Furthermore, stimulation of adipocytes with parasite lysates also suggests that a parasite factor can induce lipolysis, even in the absence of viable parasites (Figure 12). Together, this data shows that a soluble factor of parasite origin can activate lipolysis in adipocytes.

#### 4.3.1. *T. brucei*-derived factor

In co-cultures with parasite lysates, we observed a trend for increased lipolysis early post-incubation (6h) but this effect is not as obvious after 24h (Figure 12). The fact that this trend is not maintained over time with significance might be due to stability of this factor (or complex of factors) during the incubation period of the experiment.

*T. brucei* lysates encompass a complex mixture of proteins, nucleic acids (DNA and RNA) and lipids. In the case of proteins, maintaining the correct folding might be determinant to interaction with

receptors. Another aspect is exposure of potential activators of lipolysis to the parasite degradation machinery after disrupting the compartmentalization of the cell (e.g., nucleases and proteases). Or even, lability due to physical factors (e.g., media composition) or just inherent half-live of biomolecules. In the future, to identify the type of molecule(s) contributing to increased lipolysis, we could selectively remove each type of biomolecule from the parasite lysate and check variations in lipolysis. This could be achieved by enzymatically treating the lysate with proteinase K, DNase and/or RNase prior to adipocyte stimulation.

By using lysates, epitopes that would not naturally be exposed for presentation in viable parasites are available to interact with potential receptors. For example, activation of macrophages by parasite CpG DNA via TLR-9 signaling[128] is possible due to elimination/lysis of stumpy forms and release of CpG oligonucleotides into circulation[129]. Interaction of PAMPs with PRRs can also activate lipolysis. It has been demonstrated that the bacterial endotoxin (LPS) can induce adipocyte lipolysis via signaling through TLR-4[67]. 3T3-L1 adipocytes are known to be responsive to TLR-2/1, TLR-3, TLR-4, TLR-2/6 and TLR-9 agonists[65,109,110], to investigate if TLRs are involved in increase of lipolysis we could assess the release of lipolytic products in TLR-deficient 3T3-L1 adipocytes in co-culture with *T. brucei*. Alternatively, the same strategy could be employed with 3T3-L1 adipocytes deficient for either myeloid differentiation primary response 88 (Myd88) or TIR-domain-containing adapter-inducing interferon-β (TRIF), which are the downstream adapter proteins required for TLR signaling.

This soluble factor could be a consequence of parasite death or it could be actively released by the parasite. Some factors released by the parasite can modulate the host response to infection. For example, another *T. brucei* PAMP is soluble VSG (sVSG) which results from the cleavage of glycosylphosphatidylinositol (GPI)-anchored VSG by the parasite endogenous phospholipase C. sVSG activates macrophages via scavenger receptor type A[129].

### 4.3.2. *T. brucei* extracellular vesicles

Intercellular communication between *T. brucei* and surrounding host cells can also be mediated by other processes. Some protozoan parasites, including *T. brucei*, can produce and release extracellular vesicles (EVs). EVs are membrane-bound structures that can carry biological molecules and virulence factors, affecting the infection process and contributing to host modulation[130]. In *T. brucei* these structures originate from long filaments that protrude from the flagellar membrane, known as nanotubes, that then vesicularize into EVs[131]. *In vitro* production of EVs by *T. brucei* was enhanced under stress conditions (RNA interference against an essential protein) or exposure to complement active FBS[131]. *In vivo* work has shown that the number of *T. brucei* parasites in the AT (but not in the blood) is controlled by the complement system[89]. It is possible the action of the complement system in the AT enhances EV production by the parasites in this tissue.

It was also described that *T. brucei* EVs could fuse with lipid bilayers in artificial liposomes and with host RBCs, changing their physical properties and causing anemia in mice[131]. This is an example of the ability of EVs to fuse with and remodel mammalian cells. Like in the RBC, the adipocyte could be a target for *T. brucei* EVs leading to modulation of lipolysis. *T. brucei* EVs are known to carry a wide variety of both membrane bound and cytosolic proteins. Among these is VSG, the most abundant protein in *T. brucei* cell membrane. Interestingly, RBCs treated with *T. brucei* EVs show VSG on their surface, thus EVs are efficient vehicles for transfer of membrane proteins[131].

The transfer of parasite molecules by EVs into the host's adipocytes may allow for extensive modulation of the adipocyte's metabolism. This is an especially interesting prospect, as there is evidence that the parasite can hijack the host's cAMP signaling by introducing parasitic ACs into the host cell[132]. Specifically, the AC expression site-associated gene 4 (ESAG4) was implicated in cAMP-mediated activation of host PKA in liver myeloid cells probably via phagocytosed parasites[132]. Interestingly, genes related to (GR)ESAG4 (i.e., another AC) was shown to be present in *T. brucei* EVs[131].

Activation of PKA in adipocytes is a central step in lipolysis initiation. As discussed above, phosphorylation of HSL and PLIN1 is mediated by this kinase. *T. brucei* could facilitate an increase in adipocyte lipolysis through delivery of fusogenic EVs carrying GRESAG4 to adipocytes (Figure 15). Incorporation of GRESAG4 in the adipocyte plasma membrane could then lead to an increase in intracellular cAMP levels and PKA activation, provided a given stimulus (Figure 15). What triggers activation of *T. brucei* ACs is still unclear, but stress conditions like acidic environments and proteolysis have been suggested as possible activators[133,134]. Unlike mammalian ACs, which are indirectly activated by G protein-coupled receptors, trypanosome ACs, due to their topology, might have a role as surface receptors and in ligand-binding[135]. However, no potential ligands have been yet identified[135,136].

It is curious that *T. brucei* genome encodes around 80 ACs since other classical components of cAMP signaling pathways, like G protein-coupled receptors, are missing[135,137]. Some *T. brucei* ACs have been implicated in parasite cytokinesis[137], social motility[138] and response to host immune system[132], but the purpose of many others remains unclear.

### 4.3.3. *T. brucei* mechanical cue

Cells can also sense mechanical forces in their microenvironment, a process known as mechanosensing. These forces include compressive, tensile, shear stress and hydrostatic pressure but also substrate roughness, stiffness and adhesiveness[139]. This can be a receptor-mediated process and it allows physical cues to be transduced into biological responses[139]. Adipocytes are increasingly recognized as mechanosensitive and mechanoresponsive cells[140]. Early on, mechanical cues can influence suppression and promotion of adipogenesis[140]. More recently, a mechanosensitive ion channel (Piezo1) highly expressed in adipocytes, was implicated in obesity[141]. Given that *T. brucei* was found in

intricate interactions with adipocytes in the skin[22], including burial of their anterior part into the adipocyte, a mechanical force exerted by the parasite on the adipocyte surface could initiate a sequence of signaling events, interfering with lipolysis. While our data supports a model where direct physical contact is not essential for the increase in adipocyte lipolysis, mechanosensing could be an additional factor contributing to this increase since direct contact between *T. brucei* and adipocytes enhanced lipolysis.

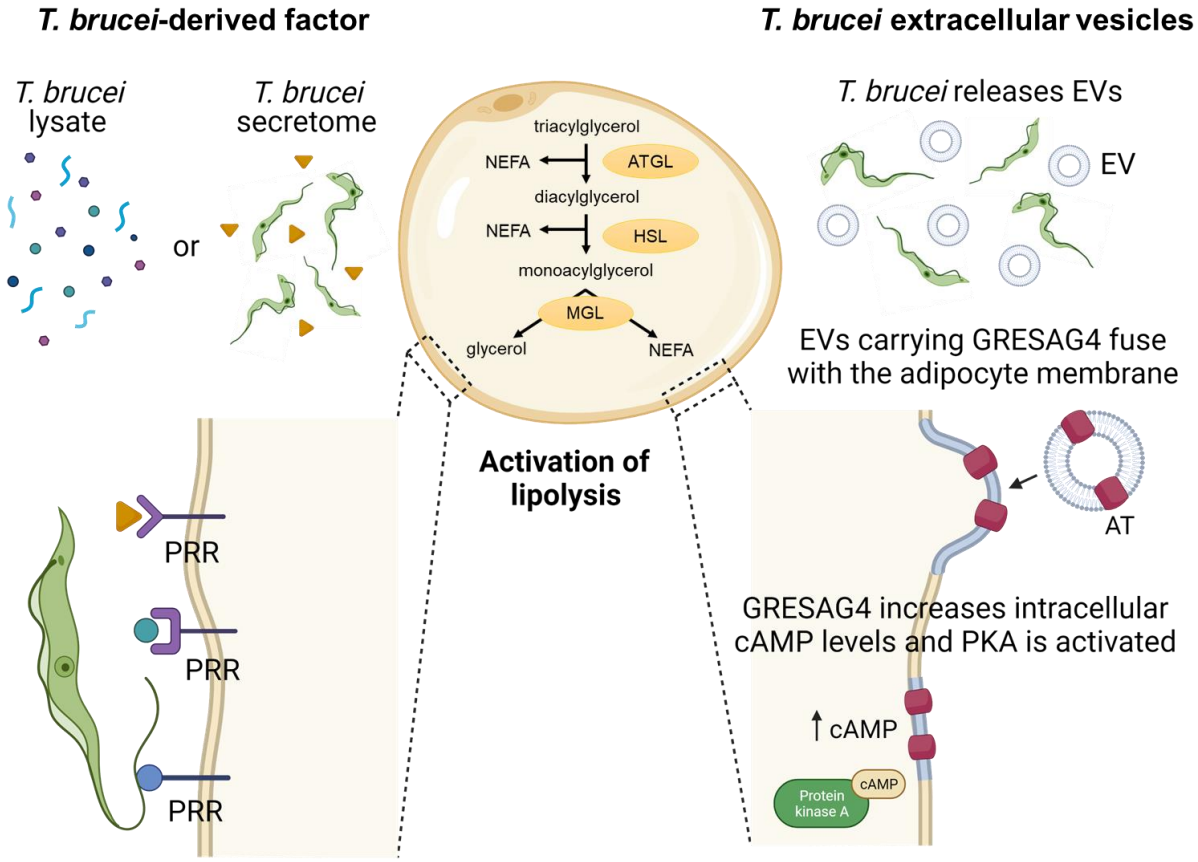


**Figure 15. Working model for adipocyte lipolysis activation by *T. brucei* during co-culture.** *T. brucei*-derived factor: Unknown factor, originated from parasite lysis or released by the parasite, binds a PRR on the surface of the adipocyte, leading to lipolysis activation. Lipolysis activation could also be mediated by direct interaction of the parasite with a PRR. *T. brucei* extracellular vesicles: EVs produced by T. brucei during co-culture with adipocytes fuse with the adipocyte plasma membrane, delivering the AT (GRESAG4). After AT activation due to an unknown stimulus, intracellular cAMP levels increase, activating PKA. PKA will then phosphorylate PLIN1 and HSL, activating lipolysis and leading to the release of lipolytic products (glycerol and NEFAs). PRR, pattern recognition receptor; EV, extracellular vesicle; AT, adenylate cyclase; cAMP, cyclic adenosine monophosphate; PKA, protein kinase A; ATGL, adipose triglyceride lipase; HSL, hormone-sensitive lipase; MGL, monoacylglycerol lipase; NEFA, non-esterified fatty acid. Created with Biorender.

## 4.4. Alternative models

Although the 3T3-L1 adipocyte cell line was chosen as our working model to study lipolysis during *T. brucei* infection, it does not encompass other aspects of AT biology (e.g., other cell populations and

paracrine interactions) that might be important during infection. The attempt to reproduce the increased lipolysis phenotype in a model closer to the *in vivo* condition was not successful (Figure 11). We used AT explants isolated from mice and infected them *in vitro* with *T. brucei*. While there is an increase in glycerol release in infected explants, NEFA release is not significantly different from non-infected explants.

Several aspects of this model must be optimized, including the diffusion of parasites into the tissue explant. This is the main limiting step in this model since we cannot guarantee proper dissemination of parasites as observed in an *in vivo* infection, through the vasculature of the AT. In the future, we could attempt to deliver the parasite inocula to the AT explant through microinjections to ensure colonization of deeper layer of the AT explant. Moreover, fragmentation of the AT explant into smaller fractions could maximize the contact area between trypanosomes and the adipocytes. Additionally, during co-culture AT explants float on top of the media which leaves the explant partially unexposed to parasites. This is another issue in co-cultures with AT explants that contributes to lack of parasite diffusion. For this, we could use a scaffolding mechanism to prevent floating and fix the explant (e.g., plates with Matrigel embedded explant[142]).

Primary preadipocytes, precursor cells present in mice WAT, can also be isolated and differentiated into mature adipocytes *in vitro.* This could also represent a suitable cellular system to validate our findings in the 3T3-L1 cell line[143]. Besides two-dimensional models, the use of more complex *in vitro* models like three-dimensional (3D) adipose spheroids could be suitable to study our hypothesis. 3D spheroid cultures have already been used in the context of protozoan infection, namely hepatic spheroids were developed to study the liver stage of *Plasmodium* spp. infection[144]. Furthermore, 3D models of adipose tissue were also applied in the study of other diseases like obesity and type 2 diabetes[145,146].

### 4.5. *T. brucei* adaptations in co-culture with adipocytes

Finally, it would be interesting to explore if and how the parasite adapts in co-culture with adipocytes. The utility to the host or *T. brucei* of NEFAs and glycerol released by the adipocyte remains elusive. Nonetheless, *T. brucei* ATFs found in mice were able to metabolize fatty acids, unlike their BSFs counterparts[18]. Furthermore, establishment of *T. brucei* in the AT may also contribute to parasite persistence behavior which is currently under investigation[147]. Besides analyzing if parasites co-cultured with 3T3-L1 adipocytes recapitulate *in vivo* ATFs by transcriptome analysis, it would be valuable to investigate how adipocyte lipolysis may modulate parasite division, differentiation and metabolism.

In summary, we have presented evidence that co-culturing *T. brucei* and 3T3-L1 adipocytes leads to an increase in adipocyte lipolysis through an ATGL-dependent mechanism. Although live parasites

are more efficient at eliciting an increase in lipolysis, a soluble factor could also be contributing to this increase.

# 5. References


1. Steverding, D. The history of African trypanosomiasis. *Parasit. Vectors* **1**, 3 (2008).
2. Stuart, K. *et al.* Kinetoplastids: related protozoan pathogens, different diseases. *J. Clin. Invest.* **118**, 1301–1310 (2008).
3. World Health Organization. Human African Trypanosomiasis (sleeping sickness) [fact sheet]. (2021). Available at: https://www.who.int/news-room/fact-sheets/detail/trypanosomiasis-human-african-(sleeping-sickness).
4. Büscher, P., Cecchi, G., Jamonneau, V. & Priotto, G. Human African trypanosomiasis. *Lancet* **390**, 2397–2409 (2017).
5. World Health Organization. Ending the neglect to attain the Sustainable Development Goals: A road map for neglected tropical diseases 2021-2030. (2021).
6. Kennedy, P. G. E. Clinical features, diagnosis, and treatment of human African trypanosomiasis (sleeping sickness). *Lancet Neurol.* **12**, 186–194 (2013).
7. Gunn, A. & Pitt, S. J. Parasitic Protozoa, Fungi and Plants: Phylum Kinetoplastida. in *Parasitology* 62–81 (John Wiley & Sons, Ltd, 2012). doi:https://doi.org/10.1002/9781119968986.ch2
8. Kennedy, P. G. E. Human African trypanosomiasis of the CNS: current issues and challenges. *J. Clin. Invest.* **113**, 496–504 (2004).
9. Lindner, A. K. *et al.* New WHO guidelines for treatment of gambiense human African trypanosomiasis including fexinidazole: substantial changes for clinical practice. *Lancet Infect. Dis.* **20**, e38–e46 (2020).
10. Simarro, P., Franco, J., Diarra, A. & Jannin, J. Epidemiology of human African trypanosomiasis. *Clin. Epidemiol.* **6**, 257–275 (2014).
11. Silva Pereira, S., Trindade, S., De Niz, M. & Figueiredo, L. M. Tissue tropism in parasitic diseases. *Open Biol.* **9**, 190036 (2019).
12. Food and Agriculture Organization. Controlling tsetse and trypanosomosis to protect African livestock keepers, public health and farmers' livelihoods. (2019).
13. Silvester, E., McWilliam, K. & Matthews, K. The Cytological Events and Molecular Control of Life Cycle Development of Trypanosoma brucei in the Mammalian Bloodstream. *Pathogens* **6**, 29 (2017).
14. Rotureau, B. & Van Den Abbeele, J. Through the dark continent: African trypanosome development in the tsetse fly. *Front. Cell. Infect. Microbiol.* **3**, 1–7 (2013).
15. Smith, T. K., Bringaud, F., Nolan, D. P. & Figueiredo, L. M. Metabolic reprogramming during the Trypanosoma brucei life cycle. *F1000Research* **6**, 683 (2017).
16. Matthews, K. R., McCulloch, R. & Morrison, L. J. The within-host dynamics of African trypanosome infections. *Philos. Trans. R. Soc. B Biol. Sci.* **370**, 20140288 (2015).
17. Rojas, F. & Matthews, K. R. Quorum sensing in African trypanosomes. *Curr. Opin. Microbiol.* **52**, 124–129 (2019).
18. Trindade, S. *et al.* Trypanosoma brucei Parasites Occupy and Functionally Adapt to the Adipose Tissue in Mice. *Cell Host Microbe* **19**, 837–848 (2016).

19. McCall, L.-I., Siqueira-Neto, J. L. & McKerrow, J. H. Location, Location, Location: Five Facts about Tissue Tropism and Pathogenesis. *PLOS Pathog.* **12**, e1005519 (2016).

20. McCall, L.-I. Quo vadis? Central Rules of Pathogen and Disease Tropism. *Front. Cell. Infect. Microbiol.* **11**, (2021).

21. Capewell, P. *et al.* The skin is a significant but overlooked anatomical reservoir for vector-borne African trypanosomes. *Elife* **5**, 1–17 (2016).

22. Caljon, G. *et al.* The Dermis as a Delivery Site of Trypanosoma brucei for Tsetse Flies. *PLOS Pathog.* **12**, e1005744 (2016).

23. Alfituri, O. A. *et al.* To the Skin and Beyond: The Immune Response to African Trypanosomes as They Enter and Exit the Vertebrate Host. *Front. Immunol.* **11**, 1–19 (2020).

24. Mogk, S. *et al.* African trypanosomes and brain infection – the unsolved question. *Biol. Rev.* **92**, 1675–1687 (2017).

25. Wolburg, H. *et al.* Late Stage Infection in Sleeping Sickness. *PLoS One* **7**, e34304 (2012).

26. Biteau, N. *et al.* Trypanosoma brucei gambiense Infections in Mice Lead to Tropism to the Reproductive Organs, and Horizontal and Vertical Transmission. *PLoS Negl. Trop. Dis.* **10**, 1–15 (2016).

27. Carvalho, T. *et al.* Trypanosoma brucei triggers a marked immune response in male reproductive organs. *PLoS Negl. Trop. Dis.* **12**, e0006690 (2018).

28. Claes, F. *et al.* Bioluminescent imaging of Trypanosoma brucei shows preferential testis dissemination which may hamper drug efficacy in sleeping sickness. *PLoS Negl. Trop. Dis.* **3**, 1–10 (2009).

29. De Niz, M. *et al.* Organotypic endothelial adhesion molecules are key for Trypanosoma brucei tropism and virulence. *Cell Rep.* **36**, 109741 (2021).

30. Capewell, P. *et al.* Resolving the apparent transmission paradox of African sleeping sickness. *PLOS Biol.* **17**, e3000105 (2019).

31. Forrester, J. V., McMenamin, P. G. & Dando, S. J. CNS infection and immune privilege. *Nat. Rev. Neurosci.* **19**, 655–671 (2018).

32. Rocha, G., Martins, A., Gama, G., Brandão, F. & Atouguia, J. Possible cases of sexual and congenital transmission of sleeping sickness. *Lancet* **363**, 247 (2004).

33. Mital, P., Hinton, B. T. & Dufour, J. M. The Blood-Testis and Blood-Epididymis Barriers Are More than Just Their Tight Junctions1. *Biol. Reprod.* **84**, 851–858 (2011).

34. Rydén, M. & Arner, P. Fat loss in cachexia—is there a role for adipocyte lipolysis? *Clin. Nutr.* **26**, 1–6 (2007).

35. Lamour, S. D. *et al.* Discovery of Infection Associated Metabolic Markers in Human African Trypanosomiasis. *PLoS Negl. Trop. Dis.* **9**, 1–17 (2015).

36. Wang, Y. *et al.* Global metabolic responses of mice to Trypanosoma brucei brucei infection. *Proc. Natl. Acad. Sci.* **105**, 6127–6132 (2008).

37. Tanowitz, H. B., Scherer, P. E., Mota, M. M. & Figueiredo, L. M. Adipose Tissue: A Safe Haven for Parasites? *Trends Parasitol.* **33**, 276–284 (2017).

38. Sudarshi, D. *et al.* Human African Trypanosomiasis Presenting at Least 29 Years after Infection—What Can This Teach Us about the Pathogenesis and Control of This Neglected Tropical Disease? *PLoS Negl. Trop. Dis.* **8**, e3349 (2014).

39. Tongue, L. K., Louis, F. & Dologuele, N. F. Relapse After Treatment with First Stage Drug in Human African Trypanosomiasis: Contribution of Molecular Biology. *Int. J. Infect. Dis.* **12**, e383 (2008).

40. Chappuis, F., Loutan, L., Simarro, P., Lejon, V. & Büscher, P. Options for Field Diagnosis of Human African Trypanosomiasis. *Clin. Microbiol. Rev.* **18**, 133–146 (2005).

41. Mudji, J. *et al.* Gambiense Human African Trypanosomiasis Sequelae after Treatment: A Follow-Up Study 12 Years after Treatment. *Trop. Med. Infect. Dis.* **5**, 10 (2020).

42. Rosen, E. D. & Spiegelman, B. M. What We Talk About When We Talk About Fat. *Cell* **156**, 20–44 (2014).

43. Choe, S. S., Huh, J. Y., Hwang, I. J., Kim, J. I. & Kim, J. B. Adipose Tissue Remodeling: Its Role in Energy Metabolism and Metabolic Disorders. *Front. Endocrinol. (Lausanne).* **7**, 1–16 (2016).

44. Schoettl, T., Fischer, I. P. & Ussar, S. Heterogeneity of adipose tissue in development and metabolic function. *J. Exp. Biol.* **221**, (2018).

45. Harms, M. & Seale, P. Brown and beige fat: development, function and therapeutic potential. *Nat. Med.* **19**, 1252–1263 (2013).

46. Kiefer, F. W. Browning and thermogenic programing of adipose tissue. *Best Pract. Res. Clin. Endocrinol. Metab.* **30**, 479–485 (2016).

47. Zhang, F. *et al.* An Adipose Tissue Atlas: An Image-Guided Identification of Human-like BAT and Beige Depots in Rodents. *Cell Metab.* **27**, 252-262.e3 (2018).

48. Athenstaedt, K. & Daum, G. The life cycle of neutral lipids: synthesis, storage and degradation. *Cell. Mol. Life Sci.* **63**, 1355–1369 (2006).

49. Lass, A., Zimmermann, R., Oberer, M. & Zechner, R. Lipolysis - A highly regulated multi-enzyme complex mediates the catabolism of cellular fat stores. *Prog. Lipid Res.* **50**, 14–27 (2011).

50. Ducharme, N. A. & Bickel, P. E. Minireview: Lipid Droplets in Lipogenesis and Lipolysis. *Endocrinology* **149**, 942–949 (2008).

51. Zechner, R., Madeo, F. & Kratky, D. Cytosolic lipolysis and lipophagy: two sides of the same coin. *Nat. Rev. Mol. Cell Biol.* **18**, 671–684 (2017).

52. Nelson, D., Cox, M. & Lehninger, A. Chapter 17: Fatty Acid Catabolism. in *Lehninger Principles of Biochemistry*. 667–693 (2012).

53. Zimmermann, R. Fat Mobilization in Adipose Tissue Is Promoted by Adipose Triglyceride Lipase. *Science (80-. ).* **306**, 1383–1386 (2004).

54. Haemmerle, G. Defective Lipolysis and Altered Energy Metabolism in Mice Lacking Adipose Triglyceride Lipase. *Science (80-. ).* **312**, 734–737 (2006).

55. Kulminskaya, N. & Oberer, M. Protein-protein interactions regulate the activity of Adipose Triglyceride Lipase in intracellular lipolysis. *Biochimie* **169**, 62–68 (2020).

56. Frühbeck, G., Méndez-Giménez, L., Fernández-Formoso, J.-A., Fernández, S. & Rodríguez, A. Regulation of adipocyte lipolysis. *Nutr. Res. Rev.* **27**, 63–93 (2014).

57. Osuga, J. -i. *et al.* Targeted disruption of hormone-sensitive lipase results in male sterility and adipocyte hypertrophy, but not in obesity. *Proc. Natl. Acad. Sci.* **97**, 787–792 (2000).

58. Haemmerle, G. *et al.* Hormone-sensitive Lipase Deficiency in Mice Causes Diglyceride Accumulation in Adipose Tissue, Muscle, and Testis. *J. Biol. Chem.* **277**, 4806–4815 (2002).

59. Nielsen, T. S., Jessen, N., Jørgensen, J. O. L., Møller, N. & Lund, S. Dissecting adipose tissue lipolysis: molecular regulation and implications for metabolic disease. *J. Mol. Endocrinol.* **52**, R199–R222 (2014).

60. Bézaire, V. & Langin, D. Regulation of adipose tissue lipolysis revisited. *Proc. Nutr. Soc.* **68**, 350–360 (2009).

61. Chen, X., Xun, K., Chen, L. & Wang, Y. TNF-α , a potent lipid metabolism regulator. *Cell Biochem. Funct.* **27**, 407–416 (2009).

62. Souza, S. C. *et al.* TNF-α induction of lipolysis is mediated through activation of the extracellular signal related kinase pathway in 3T3-L1 adipocytes. *J. Cell. Biochem.* **89**, 1077–1086 (2003).

63. Lafontan, M. & Langin, D. Lipolysis and lipid mobilization in human adipose tissue. *Prog. Lipid Res.* **48**, 275–297 (2009).

64. Rydén, M. & Arner, P. Tumour necrosis factor-α in human adipose tissue - from signalling mechanisms to clinical implications. *J. Intern. Med.* **262**, 431–438 (2007).

65. Grant, R. W. & Stephens, J. M. Fat in flames: influence of cytokines and pattern recognition receptors on adipocyte lipolysis. *Am. J. Physiol. Metab.* **309**, E205–E213 (2015).

66. Lundgren, P. & Thaiss, C. A. The microbiome-adipose tissue axis in systemic metabolism. *Am. J. Physiol. Liver Physiol.* **318**, G717–G724 (2020).

67. Zu, L. *et al.* Bacterial Endotoxin Stimulates Adipose Lipolysis via Toll-Like Receptor 4 and Extracellular Signal-regulated Kinase Pathway. *J. Biol. Chem.* **284**, 5915–5926 (2009).

68. Chi, W. *et al.* Bacterial Peptidoglycan Stimulates Adipocyte Lipolysis via NOD1. *PLoS One* **9**, e97675 (2014).

69. Morigny, P., Houssier, M., Mouisel, E. & Langin, D. Adipocyte lipolysis and insulin resistance. *Biochimie* **125**, 259–266 (2016).

70. Salehian, B. *et al.* Adenovirus 36 DNA in Adipose Tissue of Patient with Unusual Visceral Obesity. *Emerg. Infect. Dis.* **16**, 850–852 (2010).

71. Akheruzzaman, M., Hegde, V. & Dhurandhar, N. V. Twenty-five years of research about adipogenic adenoviruses: A systematic review. *Obes. Rev.* **20**, 499–509 (2019).

72. Giralt, M., Domingo, P. & Villarroya, F. Adipose tissue biology and HIV-infection. *Best Pract. Res. Clin. Endocrinol. Metab.* **25**, 487–499 (2011).

73. Munier, S., Borjabad, A., Lemaire, M., Mariot, V. & Hazan, U. In vitro infection of human primary adipose cells with HIV-1: a reassessment. *AIDS* **17**, (2003).

74. Couturier, J. & Lewis, D. E. HIV Persistence in Adipose Tissue Reservoirs. *Curr. HIV/AIDS Rep.* **15**, 60–71 (2018).

75. Giralt, M., Domingo, P. & Villarroya, F. HIV-1 Infection and the PPARγ-Dependent Control of Adipose Tissue Physiology. *PPAR Res.* **2009**, 1–8 (2009).

76. Agarwal, N. *et al.* HIV-1 Vpr Induces Adipose Dysfunction in Vivo Through Reciprocal Effects on PPAR/GR Co-Regulation. *Sci. Transl. Med.* **5**, 213ra164 (2013).

77. Faucher, J.-F. *et al.* Brill-Zinsser Disease in Moroccan Man, France, 2011. *Emerg. Infect. Dis.* **18**, 171–172 (2012).

78. Bechah, Y., Paddock, C. D., Capo, C., Mege, J.-L. & Raoult, D. Adipose Tissue Serves as a Reservoir for Recrudescent Rickettsia prowazekii Infection in a Mouse Model. *PLoS One* **5**, e8547 (2010).

79. Bechah, Y. *et al.* Persistence of Coxiella burnetii, the Agent of Q Fever, in Murine Adipose Tissue. *PLoS One* **9**, e97503 (2014).

80. Neyrolles, O. *et al.* Is Adipose Tissue a Place for Mycobacterium tuberculosis Persistence? *PLoS One* **1**, e43 (2006).

81. Daniel, J., Maamar, H., Deb, C., Sirakova, T. D. & Kolattukudy, P. E. Mycobacterium tuberculosis Uses Host Triacylglycerol to Accumulate Lipid Droplets and Acquires a Dormancy-Like Phenotype in Lipid-Loaded Macrophages. *PLoS Pathog.* **7**, e1002093 (2011).

82. Maurya, R. K., Bharti, S. & Krishnan, M. Y. Triacylglycerols: Fuelling the Hibernating Mycobacterium tuberculosis. *Front. Cell. Infect. Microbiol.* **8**, 1–8 (2019).

83. Matos Ferreira, A. V. *et al.* Evidence for Trypanosoma cruzi in adipose tissue in human chronic Chagas disease. *Microbes Infect.* **13**, 1002–1005 (2011).

84. Combs, T. P. *et al.* The Adipocyte as an Important Target Cell for Trypanosoma cruzi Infection. *J. Biol. Chem.* **280**, 24085–24094 (2005).

85. Nagajyothi, F. *et al.* Response of Adipose Tissue to Early Infection With Trypanosoma cruzi (Brazil Strain). *J. Infect. Dis.* **205**, 830–840 (2012).

86. González, F. B. *et al.* Immune response triggered by Trypanosoma cruzi infection strikes adipose tissue homeostasis altering lipid storage, enzyme profile and adipokine expression. *Med. Microbiol. Immunol.* **208**, 651–666 (2019).

87. Franke-Fayard, B. *et al.* Murine malaria parasite sequestration: CD36 is the major receptor, but cerebral pathology is unlinked to sequestration. *Proc. Natl. Acad. Sci.* **102**, 11468–11473 (2005).

88. Miller, L. H. Distribution of Mature Trophozoites and Schizonts of Plasmodium Falciparum in the Organs of Aotus Trivirgatus, the Night Monkey. *Am. J. Trop. Med. Hyg.* **18**, 860–865 (1969).

89. Machado, H. *et al.* Trypanosoma brucei triggers a broad immune response in the adipose tissue. *PLOS Pathog.* **17**, e1009933 (2021).

90. Coomassie Blue Protein Gel Stain. *Cold Spring Harb. Protoc.* **2013**, pdb.rec073924 (2013).

91. Livak, K. J. & Schmittgen, T. D. Analysis of Relative Gene Expression Data Using Real-Time Quantitative PCR and the 2−ΔΔCT Method. *Methods* **25**, 402–408 (2001).

92. RIPA Lysis Buffer. *Cold Spring Harb. Protoc.* **2017**, pdb.rec101428 (2017).

93. Bahmad, H. F. *et al.* Modeling Adipogenesis: Current and Future Perspective. *Cells* **9**, 2326 (2020).

94. Ruiz-Ojeda, F., Rupérez, A., Gomez-Llorente, C., Gil, A. & Aguilera, C. Cell Models and Their Application for Studying Adipogenic Differentiation in Relation to Obesity: A Review. *Int. J. Mol. Sci.* **17**, 1040 (2016).

95. Duszenko, M., Ferguson, M. A., Lamont, G. S., Rifkin, M. R. & Cross, G. A. Cysteine eliminates the feeder cell requirement for cultivation of Trypanosoma brucei bloodstream forms in vitro. *J. Exp. Med.* **162**, 1256–1263 (1985).

96. Hirumi, H., Doyle, J. & Hirumi, K. African trypanosomes: cultivation of animal-infective Trypanosoma brucei in vitro. *Science (80-. ).* **196**, 992–994 (1977).

97. Schweiger, M. *et al.* Chapter Ten - Measurement of Lipolysis. in *Methods of Adipose Tissue Biology, Part B* (ed. MacDougald, O. A.) **538**, 171–193 (Academic Press, 2014).

98. Forest, C. *et al.* Fatty acid recycling in adipocytes: a role for glyceroneogenesis and phosphoenolpyruvate carboxykinase. *Biochem. Soc. Trans.* **31**, 1125–1129 (2003).

99. Ho, R. & Shi, Q.-H. Forskolin as a novel lipolytic agent. *Biochem. Biophys. Res. Commun.* **107**, 157–164 (1982).

100. Dheda, K. *et al.* The implications of using an inappropriate reference gene for real-time reverse transcription PCR data normalization. *Anal. Biochem.* **344**, 141–143 (2005).

101. Dheda, K. *et al.* Validation of housekeeping genes for normalizing RNA expression in real-time PCR. *Biotechniques* **37**, 112–119 (2004).

102. Schweiger, M. *et al.* Adipose Triglyceride Lipase and Hormone-sensitive Lipase Are the Major Enzymes in Adipose Tissue Triacylglycerol Catabolism. *J. Biol. Chem.* **281**, 40236–40241 (2006).

103. Kaur, S. *et al.* Adipose-specific ATGL ablation reduces burn injury-induced metabolic derangements in mice. *Clin. Transl. Med.* **11**, (2021).

104. Anthonsen, M. W., Rönnstrand, L., Wernstedt, C., Degerman, E. & Holm, C. Identification of Novel Phosphorylation Sites in Hormone-sensitive Lipase That Are Phosphorylated in Response to Isoproterenol and Govern Activation Properties in Vitro. *J. Biol. Chem.* **273**, 215–221 (1998).

105. Daval, M. *et al.* Anti-lipolytic Action of AMP-activated Protein Kinase in Rodent Adipocytes. *J. Biol. Chem.* **280**, 25250–25257 (2005).

106. Ambele, M. A., Dhanraj, P., Giles, R. & Pepper, M. S. Adipogenesis: A Complex Interplay of Multiple Molecular Determinants and Pathways. *Int. J. Mol. Sci.* **21**, 4283 (2020).

107. Ghorbani, A. & Abedinzade, M. Comparison of In Vitro and In Situ Methods for Studying Lipolysis. *ISRN Endocrinol.* **2013**, 1–6 (2013).

108. Frayn, K. N. Adipose tissue metabolism. *Clin. Dermatol.* **7**, 48–61 (1989).

109. Kopp, A. *et al.* Innate Immunity and Adipocyte Function: Ligand-specific Activation of Multiple Toll-like Receptors Modulates Cytokine, Adipokine, and Chemokine Secretion in Adipocytes. *Obesity* **17**, 648–656 (2009).

110. Thomalla, M. *et al.* Evidence of an anti-inflammatory toll-like receptor 9 (TLR 9) pathway in adipocytes. *J. Endocrinol.* **240**, 325–343 (2019).

111. Krüger, T. & Engstler, M. Trypanosomes – versatile microswimmers. *Eur. Phys. J. Spec. Top.* **225**, 2157–2172 (2016).

112. Mayer, N. *et al.* Development of small-molecule inhibitors targeting adipose triglyceride lipase. *Nat. Chem. Biol.* **9**, 785–787 (2013).

113. Huijsman, E. *et al.* Adipose triacylglycerol lipase deletion alters whole body energy metabolism and impairs exercise performance in mice. *Am. J. Physiol. Metab.* **297**, E505–E513 (2009).

114. Nielsen, T. S. *et al.* Fasting, But Not Exercise, Increases Adipose Triglyceride Lipase (ATGL) Protein and Reduces G(0)/G(1) Switch Gene 2 (G0S2) Protein and mRNA Content in Human Adipose Tissue. *J. Clin. Endocrinol. Metab.* **96**, E1293–E1297 (2011).

115. Kralisch, S. *et al.* Isoproterenol, TNF-α, and insulin downregulate adipose triglyceride lipase in 3T3-L1 adipocytes. *Mol. Cell. Endocrinol.* **240**, 43–49 (2005).

116. Zechner, R., Kienesberger, P. C., Haemmerle, G., Zimmermann, R. & Lass, A. Adipose triglyceride lipase and the lipolytic catabolism of cellular fat stores. *J. Lipid Res.* **50**, 3–21 (2009).

117. Granneman, J. G. *et al.* Analysis of Lipolytic Protein Trafficking and Interactions in Adipocytes. *J. Biol. Chem.* **282**, 5726–5735 (2007).

118. Chaves, V. E., Frasson, D. & Kawashita, N. H. Several agents and pathways regulate lipolysis in adipocytes. *Biochimie* **93**, 1631–1640 (2011).

119. Martin, S. *et al.* Spatiotemporal Regulation of Early Lipolytic Signaling in Adipocytes. *J. Biol. Chem.* **284**, 32097–32107 (2009).

120. Saponaro, C., Gaggini, M., Carli, F. & Gastaldelli, A. The Subtle Balance between Lipolysis and Lipogenesis: A Critical Point in Metabolic Homeostasis. *Nutrients* **7**, 9453–9474 (2015).

121. Song, Z., Xiaoli, A. & Yang, F. Regulation and Metabolic Significance of De Novo Lipogenesis in Adipose Tissues. *Nutrients* **10**, 1383 (2018).

122. Ojha, S., Budge, H. & Symonds, M. E. Adipocytes in Normal Tissue Biology. in *Pathobiology of Human Disease* 2003–2013 (Elsevier, 2014). doi:10.1016/B978-0-12-386456-7.04408-7

123. Kersten, S. Physiological regulation of lipoprotein lipase. *Biochim. Biophys. Acta - Mol. Cell Biol. Lipids* **1841**, 919–933 (2014).

124. Weinstock, P. H. *et al.* Severe hypertriglyceridemia, reduced high density lipoprotein, and neonatal death in lipoprotein lipase knockout mice. Mild hypertriglyceridemia with impaired very low density lipoprotein clearance in heterozygotes. *J. Clin. Invest.* **96**, 2555–2568 (1995).

125. Gaithuma, A. K. *et al.* Lipid metabolism and other metabolic changes in vervet monkeys experimentally infected with Trypanosoma brucei rhodesiense. *J. Med. Primatol.* **41**, 75–81 (2012).

126. Huet, G. *et al.* Serum lipid and lipoprotein abnormalities in human African trypanosomiasis. *Trans. R. Soc. Trop. Med. Hyg.* **84**, 792–794 (1990).

127. Rouzer, C. A. & Cerami, A. Hypertriglyceridemia associated with Trypanosoma brucei brucei infection in rabbits: Role of defective triglyceride removal. *Mol. Biochem. Parasitol.* **2**, 31–38 (1980).

128. Drennan, M. B. *et al.* The Induction of a Type 1 Immune Response following a Trypanosoma brucei Infection Is MyD88 Dependent. *J. Immunol.* **175**, 2501–2509 (2005).

129. Stijlemans, B. *et al.* Immune Evasion Strategies of Trypanosoma brucei within the Mammalian Host: Progression to Pathogenicity. *Front. Immunol.* **7**, (2016).

130. Gavinho, B., Rossi, I. V., Evans-Osses, I., Inal, J. & Ramirez, M. I. A new landscape of host–protozoa interactions involving the extracellular vesicles world. *Parasitology* **145**, 1521–1530 (2018).

131. Szempruch, A. J. *et al.* Extracellular Vesicles from Trypanosoma brucei Mediate Virulence Factor Transfer and Cause Host Anemia. *Cell* **164**, 246–257 (2016).

132. Salmon, D. *et al.* Adenylate Cyclases of Trypanosoma brucei Inhibit the Innate Immune Response of the Host. *Science (80-. ).* **337**, 463–466 (2012).

133. Rolin, S. *et al.* Simultaneous but independent activation of adenylate cyclase and glycosylphosphatidylinositol-phospholipase C under stress conditions in Trypanosoma brucei. *J. Biol. Chem.* **271**, 10844–10852 (1996).

134. Nolan, D. P., Rolin, S., Rodriguez, J. R., Van Den Abbeele, J. & Pays, E. Slender and stumpy bloodstream forms of Trypanosoma brucei display a differential response to extracellular acidic and proteolytic stress. *Eur. J. Biochem.* **267**, 18–27 (2000).

135. Salmon, D. Adenylate Cyclases of Trypanosoma brucei, Environmental Sensors and Controllers of Host Innate Immune Response. *Pathogens* **7**, 48 (2018).

136. Alexandre, S. *et al.* Differential expression of a family of putative adenylate/guanylate cyclase genes in Trypanosoma brucei. *Mol. Biochem. Parasitol.* **43**, 279–288 (1990).

137. Salmon, D. *et al.* Cytokinesis of Trypanosoma brucei bloodstream forms depends on expression

of adenylyl cyclases of the ESAG4 or ESAG4-like subfamily. *Mol. Microbiol.* **84**, 225–242 (2012).

138. Lopez, M. A., Saada, E. A. & Hill, K. L. Insect Stage-Specific Adenylate Cyclases Regulate Social Motility in African Trypanosomes. *Eukaryot. Cell* **14**, 104–112 (2015).

139. Chen, Y., Ju, L., Rushdi, M., Ge, C. & Zhu, C. Receptor-mediated cell mechanosensing. *Mol. Biol. Cell* **28**, 3134–3155 (2017).

140. Shoham, N. & Gefen, A. Mechanotransduction in adipocytes. *J. Biomech.* **45**, 1–8 (2012).

141. Zhao, C. *et al.* Mechanosensitive Ion Channel Piezo1 Regulates Diet-Induced Adipose Inflammation and Systemic Insulin Resistance. *Front. Endocrinol. (Lausanne).* **10**, 1–9 (2019).

142. Lee, S. G. *et al.* Endothelial angiogenic activity and adipose angiogenesis is controlled by extracellular matrix protein TGFBI. *Sci. Rep.* **11**, 9644 (2021).

143. Armani, A. *et al.* Cellular models for understanding adipogenesis, adipose dysfunction, and obesity. *J. Cell. Biochem.* **110**, 564–572 (2010).

144. Chua, A. C. Y. *et al.* Hepatic spheroids used as an in vitro model to study malaria relapse. *Biomaterials* **216**, 119221 (2019).

145. Shen, J. X. *et al.* 3D Adipose Tissue Culture Links the Organotypic Microenvironment to Improved Adipogenesis. *Adv. Sci.* **8**, 2100106 (2021).

146. Klingelhutz, A. J. *et al.* Scaffold-free generation of uniform adipose spheroids for metabolism research and drug discovery. *Sci. Rep.* **8**, 523 (2018).

147. Trindade, S. *et al.* Persistence behavior in African trypanosomes during adipose tissue colonization. *Nat. Portf.* (2021).

# 6. Appendix

## 6.1. Supplementary figures

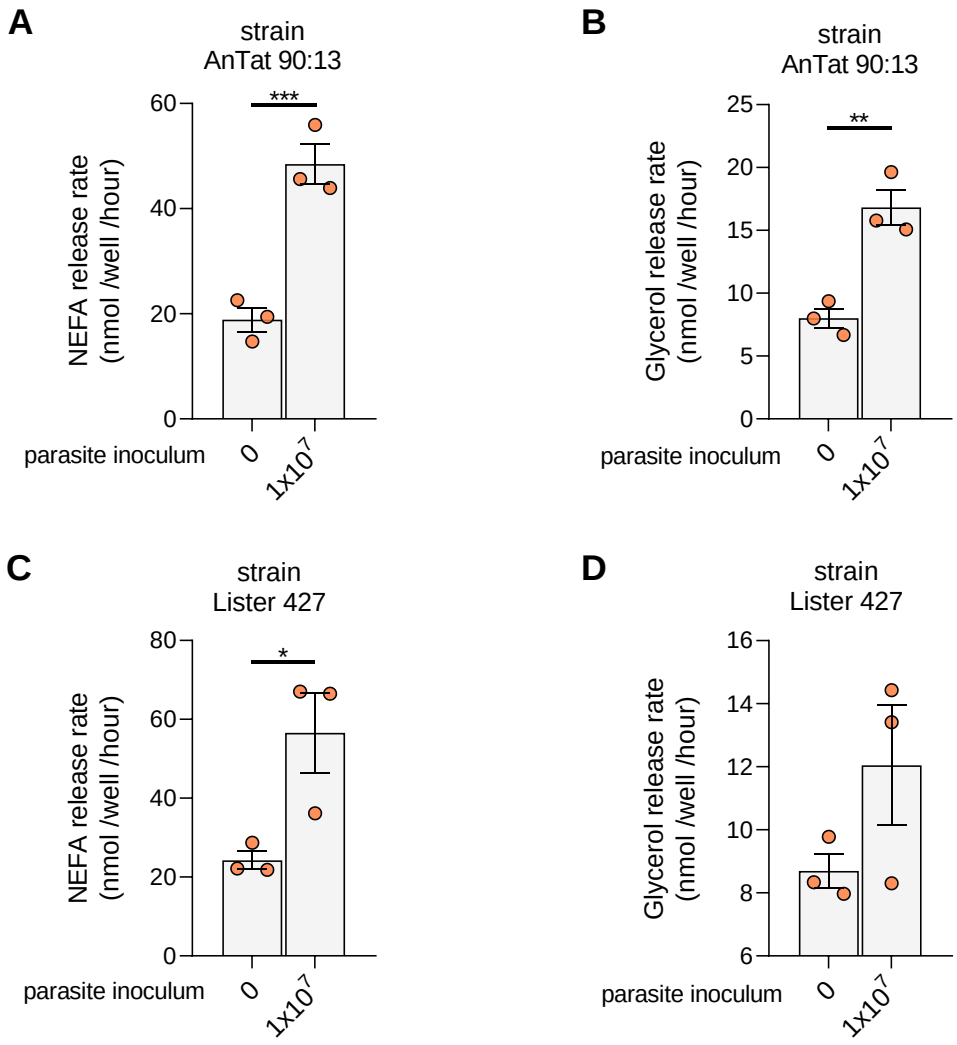


**Supplementary figure 1. Adipocyte lipolytic product release is similar in the presence of pleomorphic and monomorphic *T. brucei* strains. (A)** NEFA release rate (nmol/well/hour) of 3T3-L1 adipocytes after co-culture with *T. brucei* strain AnTat 90:13 for 24h. **(B)** Glycerol release rate (nmol/well/hour) of 3T3-L1 adipocytes after co-culture with *T. brucei* strain AnTat 90:13 for 24h. (**C)** NEFA release rate (nmol/well/hour) of 3T3-L1 adipocytes after co-culture with *T. brucei* strain Lister 427 for 24h. **(D)** Glycerol release rate (nmol/well/hour) of 3T3-L1 adipocytes after co-culture with *T. brucei* strain Lister 427 for 24h. Data are presented as mean ± SEM. One-way ANOVA with Sidak post hoc test was performed to compare experimental groups. Significance is expressed as ***$p < 0.001$, **$p < 0.01$ or *$p < 0.05$.